INFORMATION TO USERS

This manuscript has been reproduced from the microfilm master. UMI films the text directly from the original or copy submitted. Thus, some thesis and dissertation copies are in typewriter face, while others may be from any type of computer printer.

The quality of this reproduction is dependent upon the quality of the copy submitted. Broken or indistinct print, colored or poor quality illustrations and photographs, print bleedthrough, substandard margins, and improper alignment can adversely affect reproduction.

In the unlikely event that the author did not send UMI a complete manuscript and there are missing pages, these will be noted. Also, if unauthorized copyright material had to be removed, a note will indicate the deletion.

Oversize materials (e.g., maps, drawings, charts) are reproduced by sectioning the original, beginning at the upper left-hand corner and continuing from left to right in equal sections with small overlaps. Each original is also photographed in one exposure and is included in reduced form at the back of the book.

Photographs included in the original manuscript have been reproduced xerographically in this copy. Higher quality 6" x 9" black and white photographic prints are available for any photographs or illustrations appearing in this copy for an additional charge. Contact UMI directly to order.

UMI

A Bell & Howell Information Company
300 North Zeeb Road, Ann Arbor MI 48106-1346 USA
313/761-4700 800/521-0600

An Effective-Lagrangian Approach To Resummation In A Hot Scalar Theory

Alexander L. Marini
Physics Department, McGill University, Montréal

A thesis submitted to the Faculty of Graduate Studies and Research in partial fulfilment of the requirements of the degree of Doctor of Philosophy in physics.

November, 1996

Abstract

A well known feature of thermal field theories is the breakdown of the standard perturbative expansion. This breakdown is due to the appearance of the Bose-Einstein distribution which is singular in the low-momentum limit. In this thesis it is argued that an effective-Lagrangian approach can be used to restore perturbative calculability. To illustrate this point, the induced thermal mass of a scalar theory is computed to both one and two-loop order. It is shown that the results can be largely determined without the explicit evaluation of Feynman graphs. This technique is then used to calculate the finite-temperature effective potential in a scalar model with spontaneous symmetry breaking. One finds that the resummed expression for the effective potential is not valid in the region of parameter space where evidence of a first-order phase transition is observed. Therefore, contrary to some of the literature, one cannot conclude that this model exhibits a first-order phase transition.

Résumé

L'étude de la théorie des champs à température finie est caractérisée par l'échec de la théorie standard des perturbations à fournir des prédictions physiques valables. Cet effondrement du processus perturbatif est provoqué par la présence de la distribution de Bose-Einstein, laquelle est singulière pour de faibles momenta. Il est cependant proposé qu'une théorie basée sur un lagrangien effectif peut permettre de restaurer la validité de la série perturbative. Afin d'illustrer ce point, la masse thermique induite dans une théorie scalaire est calculée au premier et deuxième ordre de boucles de la série perturbative. On constate que les résultats peuvent être en grande partie obtenus sans une évaluation explicite des diagrammes de Feynman. Par conséquent, cette technique est appliquée au calcul du potentiel effectif à température finie d'un modèle scalaire avec brisure spontanée de symétrie. On constate alors que les contraintes déterminantes de la série perturbative s'obtiennent de façon simple. Cependant, on remarque aussi que l'expression pour le potentiel effectif n'est pas valide dans les régions environnantes d'une transition de phase au premier ordre. On ne peut donc pas conclure, contrairement à certaines références de la littérature actuelle, que ce modèle présente une transition de phase au premier ordre.

Statement Of Originality

Apart from the normal supervision and advice given by the thesis supervisor, the candidate has not received significant assistance from others in the preparation of this thesis. The first three chapters of the thesis serve as an introduction and review of the necessary topics that will be used throughout the thesis and therefore do not constitute original work. The computation of the induced thermal mass presented in chapters five and six reproduces known results, however, the calculation is performed efficiently within an effective-Lagrangian framework and constitutes original research. The same holds true for chapter seven. The effective potential of a scalar theory with spontaneous symmetry breaking is derived to $\mathcal{O}(1/g)$ using effective-Lagrangian techniques. The conditions governing the validity of perturbation theory near the critical point are also made explicit and can be considered as contributions to original knowledge.

Acknowledgments

There are many people to whom I would like to express my deepest thanks and appreciation. Without their support and friendship this thesis could never have been completed. First, I must thank my supervisor Cliff Burgess for his truly infinite patience and understanding. Cliff is both a talented physicist and a wonderful person. His rare combination of great insight and a crazy sense of humour makes working with him an unforgettable experience. I have learned alot from him and I wish he and his family the best.

I would like to thank my office mate Scott Hagan for the many fun and useful conservations that we have shared over the past five years. Scott has a very wide range of interests which made him the most useful reference book in our office. Scott's kindness is unmatched and if anybody deserves to live one hundred years, it is Scott. Then there's Graham Cross. Graham has turned out to be one of the best friends I've ever had in under two years. Now that's an achievement! I would like to thank him for the many conversations, dinners, lunches, movies and pool games that have made my life richer. I must also thank all the "boyz" of room 308 which inlcude Dave, Dean (Hey coach, Remember THE CATCH!), Kostas, Reiner, Andreas, Francois and Niri for their exceptional office hospitality. Free of charge, they serve you food and drink and supply you with a newspaper and a comfortable chair. Truly a five-star establishment!

Charles Hooge and Sean Pecknold deserve a special mention for allowing me to "surf the net" on their machines and for teaching me the finer points of baseball, music and Thomson House etiquette. Hey Charles.....It's Gotta Work! To Declan, Andy and J.D., thanks for introducing me to "St. Laurent Bifteck" and for proving without a doubt that smoked-meat sandwiches do taste better at 4 o'clock...in the morning! To Bao and Noureddine, thank you for all the great jokes and discussions. Studying for the preliminary exam could not have been more fun.

My stomach would like to thank Jason Breckenridge, Martin Kamela, Chris Roderick, Phil LeBlanc and May Chiao for inviting me into their homes and treating me to some of the greatest feasting experiences of my life. Jake, thanks for the

opera, movies, dinners and friendship. Martin...thanks for my new nickname and for explaining who "REALLY" has the power in PGSS. Chris...you are right...there is a Santa Claus. Phil...you have the greatest laugh of all time..."SCAN IT!". May...you have been my greatest student...only you and I understand the real meaning of "The Chicken". I must also thank all the members of "The Gourmet Club". It is always a pleasure to spend time with great friends who enjoy the same things in life.

I must thank my friends Bob Petrovic and Mhairi Stein for one of the most fun summers in recent memory. Bob, you are a great friend and your "philosophy of life" is the healthiest one I've ever experienced. I would like to thank Mhairi for introducing me to the Scottish culture through "IRN-BRU", "Drambuie", "Haggis" and other fine Scottish treats. Together you make the best housemates anyone could ever ask for.

I do not know where to begin in thanking Sean and Bonnie Punch. Their place has been like a second home...cats and all. Sean is an amazing friend and I am very grateful to him for being there when I needed him. I thank Bonnie for her friendship and the many dinner invitations. I must say that her "Christmas baking" is second to none. I look forward to our next lunch at Fry's and Co., Halifax, Nova Scotia. A special thanks to Pat Silas for being a good friend and for her company at Thomson House. Conversations with Pat are always very fun and her smile always uplifting. Thanks Pat.

I thank Ingrid Johnsrude for her love and support through part of my graduate studies and sincerely hope she can find happiness in her endeavours. I would also like to thank Suzanne Patterson for being the "bright little star". I was very lucky to meet a person like you and I'm very happy that we've become friends. I look forward to your E-mail everyday. I must also thank Rahma Tabti for being such a terrific companion over the summer. I hope I was able to bring some fun back into your life as you did to mine.

I must say "grazie" to my loving mother Nerina and sister Gianna. Throughout my studies they have continued to support and encourage me even if they weren't quite sure "what the hell I'm doing". Once again, thank you very much.

I would like to thank Denis Michaud for doing such a fine job in translating my abstract into the French language. A million thanks go out to Nancy Brown, Paula Domingues, Diane Koziol, Joanne Longo and especially Lynda Corkum for running the Physics Department, McGill University, the City of Montréal and who knows what else? Last, but not least, I would like to thank Les Fonds F.C.A.R. and the Walter C. Sumner Memorial Foundation for financial support and thank the department for support through a Dow-Hickson Scholarship.

In loving memory of Lorenzo Marini, 1931-1987.

Contents

Abstract i

Résumé ii

Statement Of Originality iii

Acknowledgments iv

Dedication vii

Table of Contents viii

List of Figures xi

1. Introduction 1

    1.1. General Introduction 1

    1.2. The Problem of Infrared Divergences 3

    1.3. Description of the Thesis 4

2. Review of Quantum Field Theory 6

    2.1. Quantum Field Theory at Zero Temperature 6

        2.1.1. The Generating Functional 6

        2.1.2. Feynman Rules For The Computation of Graphs 8

        2.1.3. Generating Functional for Connected Graphs 9

        2.1.4. One-Particle Irreducible Graphs and the Effective Action 10

        2.1.5. The Effective Potential at One-Loop Order. 13

    2.2. Quantum Field Theory at Finite Temperature 14

        2.2.1. The Partition Function 14

        2.2.2. The Finite-Temperature Feynman Rules 17

2.2.3. The Helmholtz Free Energy 18

2.2.4. High-Temperature Symmetry Restoration and the Effective Potential 20

3. The Effective Lagrangian and the Renormalization Group 23

3.1. Scalar Field Theory with a Momentum Cutoff 23

3.2. Integrating Over The High-Frequency Modes 24

3.3. The Renormalization-Group Equation 27

4. Estimating the Strengths of Effective Interactions 30

4.1. Contact Interactions 30

4.2. Derivative Interactions 33

5. The Induced Thermal Mass at One-Loop Order 37

5.1. The Standard Method 37

5.2. The Effective-Lagrangian Approach 41

5.2.1. Using the Renormalization-Group Equation 44

5.2.2. The Explicit Calculation 45

6. The Induced Thermal Mass at Two-Loop Order 48

6.1. Deriving The Effective Theory 48

6.1.1. Corrections to the Two-Point Function 49

6.1.2. Corrections to the Four-Point Function 50

6.1.3. The Effective Six-Point Interaction 51

6.2. Calculating The Induced Thermal Mass 53

6.2.1. Extracting The Coefficient of The Logarithmic Term 56

6.2.2. The Final Result 59

7. The Finite-Temperature Effective Potential 61

7.1. Scalar Theory with a Spontaneously-Broken Symmetry 61

7.2. Deriving The Effective Theory 63

7.3. Next-To-Leading Order Contributions to the Effective Potential 65

7.3.1. The High-Frequency Contribution 65

7.3.2. The Low-Frequency Contribution 68

7.4. Calculation of the Effective Potential 69

7.5. The Effective Potential as a Function of Temperature 72

7.6. Mathematical Limitations of the Result 75

8. Conclusion 78

References 81

List of Figures

Figure 2.1.1. One-loop contributions to the effective potential. 13

Figure 2.2.1. Diagrams contributing to the free energy. 19

Figure 3.2.1. Scattering diagram in ϕ^4 theory. 25

Figure 3.2.2. Graphical Interpretation of the Effective Interactions. 27

Figure 4.1.1. L-loop ring diagram with n external lines. 32

Figure 4.2.1. 1-loop corrections to the four-point function. 35

Figure 5.1.1. One-loop mass correction. 37

Figure 5.1.2. Two-loop mass corrections. 38

Figure 5.1.3. Ring-graph contribution to the two-point vertex. 39

Figure 6.1.1. Corrections to the two-point function. 49

Figure 6.1.2. Corrections to the four-point function. 50

Figure 6.1.3. Six-particle scattering in ϕ^4 theory. 51

Figure 6.2.1. One-loop and two-loop corrections to the two-point funtion in the effective theory. 54

Figure 7.2.1. One-loop corrections to the tree-level vertices. 63

Figure 7.3.1. Interaction veritices in the shifted theory. 66

Figure 7.3.2. Contributions to the effective potential from the high-energy theory. 68

Figure 7.5.1. Graph of Eq. (7.5.8). 74

Figure 7.5.2. Graph of first-order phase transition in scalar model. 75

Chapter 1.
Introduction

The purpose of this thesis is to illustrate that the perturbative expansion of thermal-field theories can be reorganized by using an effective-Lagrangian approach based on Wilson's definition of the effective action. To help the reader understand the motivation for studying this topic, a general introduction is included. The introduction reviews some of the triumphs of zero-temperature field theory and presents reasons for investigating field theories at finite-temperature and density. A section describing the problem of infrared divergences found in thermal field theories is then given to show the need for reorganizing the standard perturbative expansion. Some methods for reorganizing the perturbative expansion are reviewed and finally a section outlining the layout of the thesis is given.

1.1. General Introduction

A great triumph of modern physics is the development of Quantum Field Theory (QFT). QFT has proven to be an excellent framework for describing the fundamental particles of matter and the interactions thereof. Due to the mathematical complexity of these theories, exact solutions to the equations of motion of physical systems are difficult to obtain. In order to calculate the predictions of a theory, simplifying assumptions must be made.

A very fruitful simplifying assumption is that the coupling constants of the theory are small, $g_i \ll 1$, and therefore one can make a perturbative expansion in powers of the coupling constants. The first major achievement of QFT was the development of Quantum Electrodynamics (QED) and since the coupling constant of QED is small, $g_e = \sqrt{4\pi\alpha}$ where $\alpha \simeq \frac{1}{137}$ is the fine structure constant, perturbative calculations can be made. The amazing agreement between the prediction of perturbative QED and experiment for the magnetic moment of the electron[1] gives one confidence in both the correctness of the theory and the validity of the simplifying assumptions. QED has also correctly predicted the differential cross-sections

for Rutherford and Bhabba scattering[2] and predicted the Lamb shift[3] along with many other successes too many to mention.

Other QFT's have been developed and their successes have been very encouraging. The Electro-Weak theory of Glashow, Weinberg and Salam[4–6] is in excellent experimental agreement and provides a unifying framework to understand both the electromagnetic and weak-nuclear interactions. For example, the prediction of elastic Neutrino-Electron scattering via the neutral weak interactions is in good agreement with the experimental results[7]. The measured lifetimes of both Muons and Pions are also in agreement with the predicted results. Quantum Chromodynamics (QCD), the accepted theory of the strong interactions, has also enjoyed many successes. The approximate scaling observed in deep-inelastic scattering of Leptons off Hadrons can be explained using asymptotic freedom. Deviations at high-energy from this scaling have been predicted by QCD and are consistent with the observed scaling, given the large error in the measurements[8]. Other predictions of QCD include the narrow width of Charmonium and the existence of Quark and Gluon jets. QCD is consistent with all of the phenomenology of the strong interactions and explains much of the observed behaviour.

A feature that is shared by all of the above tests of the various QFT's is that the system in question involves only a small number of particles. A one-particle system is considered in both lifetime and magnetic-moment calculations and usually two-particle systems are studied for the scattering experiments. In order to further test these theories, one must investigate systems with a large number of particles. Thus the QFT's need to be studied at finite temperature and density.

Nonrelativistic QFT of many-partcle systems has proven to be an indispensable tool in condensed matter physics. Theories of superconductivity and superfluidity have been created using nonrelativistic QFT and have been very successful[9]. The modern theory of critical phenomena also uses the language of QFT to explain the scaling laws associated with second-order phase transitions and to calculate the critical exponents of these scaling laws. The predictions of relativistic high-temperature QFT's could be tested in at least three new domains. First there may exist significant high-temperature effects within neutron stars where the density

is considerably greater than nuclear density. The second possibility is in heavy-ion collisions at very high energy per nucleon, in which states of high density and temperature might be formed. Finally the standard cosmological models allow one to extrapolate back to times when the universe was at a temperature comparable to nucleon rest energies in units where $c = \hbar = k_B = 1$. It is hoped that QFT's at high temperature might provide some predictions concerning the evolution of the universe. Thus new insights into the nature of matter at very high temperature and density might be gained by studying relativistic QFT's at finite temperature and density.

1.2. The Problem of Infrared Divergences

A feature of perturbative calculations at finite temperature that has been recognized for many years is its severe infrared divergent behaviour. The infrared divergences found in zero-temperature field theory in $(3 + 1)$ dimensions are generically only logarithmic. The same is not true at finite temperature due to the appearance of the Bose-Einstein distribution function, $n(k) = (e^{\frac{k}{T}} - 1)^{-1}$. The Bose-Einstein distribution function behaves like T/k for small momentum k, thus the potential arises for infrared divergences to grow like a power of the infrared cutoff, rather than a logarithm. Due to these severe infrared divergences, the correspondence between the loop expansion and the coupling-constant expansion is lost and an infinite number of Feynman diagrams may contribute to a given order in the coupling-constant expansion[10].

An important example of the breakdown of the standard perturbative expansion is in the calculation of the Quark and Gluon damping rates in hot QCD. One finds that the naive application of the standard zero-temperature Feynman rules at one-loop order yields gauge-dependent results[11–12]. The reason why this one-loop calculation of the Quark and Gluon damping rates is gauge dependent is that the calculation is incomplete. Feynman diagrams of two-loop order and higher that contribute to $\mathcal{O}(g^2)$ have been neglected. In order to restore perturbative calculability, a reorganization of the perturbative expansion is required.

Methods of reorganizing the perturbative expansion of finite-temperature field theories have been developed. In particular, a method for resumming Hot QCD has been devised by Braaten and Pisarski[13]. In their analysis, they show that it is necessary to distinguish between hard momenta (momenta of the order T where T is the temperature of the plasma) and soft momenta (momenta of the order gT where g is the QCD coupling constant). When the momentum flow through a particular line in a Feynman graph is hard, ordinary perturbation theory using bare propagators and vertices can be used. If, however, the momentum is soft, then dressed propagators and vertices must be employed. Using this resummation scheme, physically sensible gauge-independent Quark and Gluon damping rates can be calculated[11,14]. An effective action which generates the Braaten-Pisarski resummed propagators and vertices has been developed which allows one to derive the Braaten-Pisarski Feynman rules in a straightforward fashion rather than by studying the contributions of diagrams on an individual basis[15–17].

An excellent illustration of the resummation technique developed by Braaten and Pisarski, applied to a scalar field, is given by Parwani[18]. In his paper, the induced thermal mass of a hot scalar field is computed to $\mathcal{O}(g^4)$. The reorganization of the perturbative expansion is achieved by the addition of the induced thermal mass to the unperturbed sector of the Lagrangian and the subtraction of the same mass from the perturbative sector. The addition and subtraction of the thermal mass term ensures that the physics described by the new Lagrangian is identical to that of the original massless theory. A reorganization of the perturbative expansion can also be achieved in a very efficient way by using an effective-Lagrangian approach based on Wilson's formulation of the effective action[19–20].

1.3. Description of the Thesis

The goal of this thesis is threefold. First, to show that one can use a renormalization-group approach to determine the contributions to the induced thermal mass from the low-energy theory without the explicit evaluation of Feynman graphs. This method also allows one to extract the non-analytic dependence on the coupling

constant which, in some cases, is numerically the most important contribution. Second, to evaluate the effective potential in a theory with spontaneous symmetry breaking and study symmetry restoration at high temperatures. Finally, to show that within a scalar field theory context the Braaten-Pisarski resummation can be understood in an effective field theory framework.

This thesis is organized in the following way. In chapter two, a review of QFT at both zero and finite temperature is presented. In chapter three a method by which the effective Lagrangian for a scalar field theory can be obtained by integrating over high-frequency modes is given. The renormalization-group equation satisfied by the bare and renormalized vertex functions is also developed. Chapter four presents some simple power-counting arguments which allow one to estimate the sizes of the contact and derivative interactions found in the effective theory. The induced thermal mass is calculated to one-loop order in chapter five using both the standard approach and the effective Lagrangian approach. Both methods are given to illustrate the usefulness of the techniques presented. The analysis of the induced thermal mass is extended to two-loop order in chapter six. In chapter seven, the effective-Lagrangian approach is employed to calculate the effective potential of a hot scalar field with spontaneous symmetry breaking. Finally, in chapter eight, the conclusions are summarized.

Chapter 2.
Review of Quantum Field Theory

The purpose of this chapter is to review some of the key concepts of Quantum Field Theory at both zero and finite temperature. It is assumed that the reader is already familiar with both of these subjects. If a more rigorous treatment of the subjects is required then the following references are recommended[21-22].

2.1. Quantum Field Theory at Zero Temperature

2.1.1. The Generating Functional

In Quantum Field Theory one is usually interested in calculating the time-ordered product of operators in the vacuum state. For instance, the quantities of interest are correlation functions of the form

$$\langle \phi(t_1, \mathbf{x}_1)\, \phi(t_2, \mathbf{x}_2) \cdots \phi(t_n, \mathbf{x}_n) \rangle$$

where the operators ϕ are time ordered such that $t_1 > t_2 > \cdots > t_n$. For simplicity, we will assume that the field ϕ is a scalar field and that the time and space coordinates $(t_i, \mathbf{x}_i)$ have a Euclidean-space signature. To regain the time-ordered products in Real-Time or Minkowski-space, one must analytically continue the Imaginary-Time or Euclidean-space correlation functions back into Minkowski-space[23]. A general method for relating the Imaginary-Time Green's functions to the Real-Time Green's functions has been developed by Evans[24]. Static quantities, such as the mass, are obtained easily in the Imaginary-Time formalism. Dynamic quantities, however, such as transport coefficients, must either be calculated directly in the Real-Time formalism or obtained by analytic continuation from the Imaginary-Time expressions.

To evaluate these correlation functions, one needs to calculate path integrals of the form

$$\langle \phi(x_1)\, \phi(x_2) \cdots \phi(x_n) \rangle = \frac{\int \mathcal{D}\phi [\phi(x_1)\, \phi(x_2) \cdots \phi(x_n)] \, exp\left(\int d^4x \mathcal{L}(\phi)\right)}{\int \mathcal{D}\phi \; exp\left(\int d^4x \mathcal{L}(\phi)\right)} \quad (2.1.1)$$

where the field ϕ on the right-hand side of Eq. (2.1.1) represents the classical scalar field ϕ and $\mathcal{L}(\phi)$ is the classical Lagrangian density. Thus all expectation values of the time-ordered products are expressed as the moments of distributions of classical fields.

An elegant method for computing the path integral can be developed by introducing a source term into the Lagrangian density $\mathcal{L}(\phi)$. By adding the term $J(x)\phi(x)$ to the classical Lagrangian density $\mathcal{L}(\phi)$, one can define the generating functional $\mathcal{Z}(J)$ as

$$\mathcal{Z}(J) = \int \mathcal{D}\phi \; exp \int d^4x \left(\mathcal{L}(\phi) + J(x)\phi(x)\right) . \tag{2.1.2}$$

The n-point coordinate-space Green's functions $G^n(x_1, \cdots, x_n)$ which are defined as

$$G^n(x_1, \cdots, x_n) = \langle \phi(x_1)\phi(x_2)\cdots\phi(x_n)\rangle \tag{2.1.3}$$

are related to the generating functional $\mathcal{Z}(J)$ by repeated functional derivatives with respect to the source term $J(x)$:

$$G^n(x_1, \cdots, x_n) = \frac{1}{\mathcal{Z}(J)} \frac{\delta^n \mathcal{Z}(J)}{\delta J(x_1)\delta J(x_2)\cdots\delta J(x_n)}\Big|_{J=0} . \tag{2.1.4}$$

If one is interested in translation-invariant theories, then it is convenient to perform all calculations in momentum space. This is achieved by substituting the Fourier transforms† of the field $\phi(x)$ and source term $J(x)$

$$\phi(x) = \mathcal{V}^{1/2} \int \frac{d^4p}{(2\pi)^2} e^{ip\cdot x}\phi(p) \tag{2.1.5a}$$

$$J(x) = \mathcal{V}^{1/2} \int \frac{d^4p}{(2\pi)^2} e^{ip\cdot x} J(p) \tag{2.1.5b}$$

into Eq. (2.1.1) and Eq. (2.1.4) where $\mathcal{V}$ is the space-time volume. The coordinate-space Green's functions are related to the momentum-space Green's functions by the equation

$$G^n(x_1, \cdot\cdot, x_n) = (2\pi)^{-2n}\mathcal{V}^{n/2} \int \prod_{j=1}^{n} d^4p_j e^{i(p_1\cdot x_1 + \cdots + p_n\cdot x_n)} G^n(p_1, \cdot\cdot, p_n)\, \delta^{(4)}\left(\sum_j p_j\right) \tag{2.1.6}$$

† The space-time volume of $\mathcal{V}$ has been included so that the mass dimension of $\phi(x)$ is one and the mass dimension of $\phi(p)$ is negative one. For simplicity, the volume can be omitted and reconstituted by dimensional analysis.

where $G^n(p_1,\cdots,p_n)$ is the n-point momentum-space Green's function defined by

$$G^n(p_1,\cdots,p_n) = \langle \phi(p_1)\,\phi(p_2)\cdots\phi(p_n)\rangle\,. \tag{2.1.7}$$

Once again, the functions $G^n(p_1,\cdots,p_n)$ can be calculated by taking functional derivatives of $\mathcal{Z}(J)$ with respect to the source term $J(-p)$:

$$G^n(p_1,\cdots,p_n) = \frac{1}{\mathcal{Z}(J)}\frac{\delta^n\mathcal{Z}(J)}{\delta J(-p_1)\,\delta J(-p_2)\cdots\delta J(-p_n)}\Big|_{J=0}\,. \tag{2.1.8}$$

2.1.2. Feynman Rules For The Computation of Graphs

Diagrammatic techniques or Feynman rules can be developed[25] to aid in the evaluation of the Green's functions. The Lagrangian density of the theory is given by

$$\mathcal{L} = \mathcal{L}_0 + \mathcal{L}_{int} \tag{2.1.9}$$

where $\mathcal{L}_0$ is the "free" or "unperturbed" sector. We assume that the interaction-Lagrangian density $\mathcal{L}_{int}$ can be expressed as

$$\mathcal{L}_{int} = -\sum_j \frac{\lambda_j}{j!}\phi^j \tag{2.1.10}$$

with the λ_j representing the coupling-constants of the theory.

With each Green's function $G^n(p_1,\cdots,p_n)$ one can associate an infinite number of graphs with n external legs where each of the n momenta are assumed to flow along one of the external legs. Thus, to calculate a Green's function to a particular order in the coupling-constant, one must determine the appropriate number and type of interaction vertices required. Once this is done, one can calculate, order by order, the contributions to the Green's function.

With each interaction of type j one associates a vertex with j external lines. One must then draw all possible graphs with a total of n external legs by connecting the lines to other vertices or leaving them unconnected to serve as the external legs. To evaluate the contribution of each graph, one associates a factor of $-\lambda_j/j!$ with each vertex of type j and a function $G(k)$ for each line carrying momentum k. It is

important to note that momentum is conserved at every vertex. The function $G(k)$ is called the free propagator and is given by

$$G(k) = \frac{1}{k^2 + m^2} \tag{2.1.11}$$

for a scalar field of mass m. To account for the indistinguishability of vertices, there is a factor of $1/n_j!$, where n_j is the number of vertices of type j. There is also an overall symmetry factor which counts all the possible ways in which a graph could have been constructed without changing its topology.

To calculate the value of a graph, one multiplies all of the above factors together and then integrates over all of the independent momenta by including a factor of the form

$$\int \frac{d^4k_l}{(2\pi)^4}$$

for each of the independent momenta k_l.

The set of graphs which contributes to $G^n(p_1, \cdots, p_n)$ includes both connected and disconnected graphs. The set of diagrams which contains vacuum graphs (graphs without external legs) does not contribute to the Green's functions. It can be shown that dividing by $\mathcal{Z}(0)$, as shown in Eq. (2.1.8), is equivalent to eliminating all graphs with vacuum pieces[26]. In summary, $G^n(p_1, \cdots, p_n)$ receives contributions from both connected and disconnected graphs with the exception of graphs with vacuum diagrams.

2.1.3. Generating Functional for Connected Graphs

The fact that $\mathcal{Z}(J)$ is the generating functional for the Green's functions implies that one can expand $\mathcal{Z}(J)$ in a Taylor series of the sources J:

$$\mathcal{Z}(J) = 1 + \sum_{n=1}^{\infty} \frac{1}{n!} \int \prod_{i=1}^{n} d^4p_i G^n(p_1, \cdots, p_n) J(-p_1) \cdots J(-p_n) \delta^{(4)}\left(\sum_i p_i\right) . \tag{2.1.12}$$

Similarly, one can define the generating functional for the connected Green's functions as

$$\mathcal{W}(J) = \sum_{n=1}^{\infty} \frac{1}{n!} \int \prod_{i=1}^{n} d^4p_i G_c^n(p_1, \cdots, p_n) J(-p_1) \cdots J(-p_n) \delta^{(4)}\left(\sum_i p_i\right) . \tag{2.1.13}$$

It can be shown[26] that the generating functionals $\mathcal{Z}(J)$ and $\mathcal{W}(J)$ are related through the equation

$$\mathcal{Z}(J) = exp(\mathcal{W}(J)) \tag{2.1.14}$$

which allows one to generate the connected Green's functions by using

$$G_c^n(p_1, \cdots, p_n) = \frac{\delta^n \log \mathcal{Z}(J)}{\delta J(-p_1)\,\delta J(-p_2)\cdots\delta J(-p_n)}\Big|_{J=0} . \tag{2.1.15}$$

The set of graphs which contribute to $G_c^n(p_1, \cdots, p_n)$ includes diagrams which are one-particle irreducible. If the propagators on the external legs of these graphs are "amputated" or "truncated" then one obtains the one-particle irreducible (1PI) vertex functions. This is a very important subset of graphs for they contain the quantum corrections to the tree-level vertices and provide a framework for treating problems with symmetry breaking in the presence of interactions.

2.1.4. One-Particle Irreducible Graphs and the Effective Action

The generating functional for the (1PI) vertex functions is related to the generating functional $\mathcal{W}$ through a Legendre transformation[27]. Although, a proof of this statement will not be given here, some examples of how the effective action generates the (1PI) vertex functions will be given.

First one must define the Legendre transform of $\mathcal{W}(J)$ with respect to the expectation value of $\langle\phi(x)\rangle = \bar{\phi}$. This is given by

$$\Gamma(\bar{\phi}) = \int d^4x \bar{\phi}(x) J(x) - \mathcal{W}(J) . \tag{2.1.16}$$

From Eq. (2.1.16) it immediately follows that

$$\frac{\delta\Gamma(\bar{\phi})}{\delta\bar{\phi}(x)} = -\int d^4y \frac{\delta\mathcal{W}(J)}{\delta J(y)}\frac{\delta J(y)}{\delta\bar{\phi}(x)} + J(x) + \int d^4y \bar{\phi}(y)\frac{\delta J(y)}{\delta\bar{\phi}(x)} = J(x) \tag{2.1.17}$$

where we have used the fact that

$$\frac{\delta\mathcal{W}(J)}{\delta J} = \bar{\phi} . \tag{2.1.18}$$

Thus the vacuum of the theory, in the absence of external sources, is defined by

$$\frac{\delta\Gamma(\bar{\phi})}{\delta\bar{\phi}}\Big|_{J=0} = 0 \tag{2.1.19}$$

which implies that the condition for a broken symmetry is

$$\frac{\delta\Gamma\left(\bar{\phi}\right)}{\delta\bar{\phi}}\Big|_{\bar{\phi}\neq 0} = 0\,. \tag{2.1.20}$$

To illustrate the how the effective action $\Gamma(\bar{\phi})$ generates the (1PI) vertex fuctions, we begin by differentiating Eq. (2.1.17) by $\bar{\phi}(y)$ which yields

$$\frac{\delta^2\Gamma\left(\bar{\phi}\right)}{\delta\bar{\phi}\left(y\right)\delta\bar{\phi}\left(x\right)} = \frac{\delta J\left(x\right)}{\delta\bar{\phi}\left(y\right)}\,. \tag{2.1.21}$$

To determine what the right-hand side of Eq. (2.1.21) represents, consider the expression $\frac{\delta\bar{\phi}(y)}{\delta J(x)}$. From Eq. (2.1.18) we know that this represents the connected two-point function $G_c(x,y)$. Therefore the right-hand side of Eq. (2.1.21) is the inverse of the connected two-point function in the sense that

$$\int d^4z \frac{\delta^2\Gamma\left(\bar{\phi}\right)}{\delta\bar{\phi}\left(x\right)\delta\bar{\phi}\left(z\right)}\frac{\delta^2\mathcal{W}\left(J\right)}{\delta J\left(z\right)\delta J\left(y\right)} = \delta^{(4)}\left(x-y\right)\,. \tag{2.1.22}$$

It can be shown that the inverse of the connected two-point function is one-particle irreducible[25]. By taking repeated functional derivatives of Eq. (2.1.22) with respect to some source J, using the definition of the connected two-point function, and using Eq. (2.1.22), one finds that

$$\Gamma^n\left(x_1,\cdots,x_n\right) = \frac{\delta^n\Gamma\left(\bar{\phi}\right)}{\delta\bar{\phi}\left(x_1\right)\delta\bar{\phi}\left(x_2\right)\cdots\delta\bar{\phi}\left(x_n\right)}\Big|_{J=0} \tag{2.1.23}$$

where $\Gamma^n(x_1,\cdots,x_n)$ is the (1PI) n-point vertex function.

Now that it has been established that $\Gamma(\bar{\phi})$ is the generating functional for the (1PI) vertex functions, one can express $\Gamma(\bar{\phi})$ in a Taylor expansion as

$$\Gamma\left(\bar{\phi}\right) = \sum_{n=0}^{\infty}\frac{1}{n!}\int\prod_{i=1}^{n}d^4x_i\Gamma^n\left(x_1,\cdots,x_n\right)\bar{\phi}\left(x_1\right)\cdots\bar{\phi}\left(x_n\right)\,. \tag{2.1.24}$$

If we assume that $\bar{\phi}(x)$ is translationally invariant so that

$$\bar{\phi}\left(x\right) = v \tag{2.1.25}$$

then one can rewrite Eq. (2.1.24) by substituting the Fourier transform of Γ^n and obtain

$$\Gamma\left(v\right) = \sum_{n=0}^{\infty}\frac{1}{n!}v^n\Gamma^n\left(0,\cdot,0\right)\int d^4x \tag{2.1.26}$$

where the Dirac delta function has been defined as

$$\delta^{(4)}(x) = \int \frac{d^4p}{(2\pi)^4} e^{ipx} \ . \tag{2.1.27}$$

The effective potential $V_{eff}(v)$, which corresponds to the internal energy of the system as a function of v, is defined as

$$\Gamma(v) = -\int d^4x V_{eff}(v) \ . \tag{2.1.28}$$

Finally, using Eq. (2.1.26) and Eq. (2.1.28), we find that the effective potential for the system of interest is given by

$$V_{eff}(v) = -\sum_{n=0}^{\infty} \frac{1}{n!} v^n \Gamma^n(0, \cdots, 0) \ . \tag{2.1.29}$$

Eq. (2.1.29) is an expression for the effective potential that can be used for explicit calculations.

One must be careful in using the Taylor expansion given by Eq. (2.1.24). The coefficients in the expansion are evaluated at $J = 0$, however, the expansion parameter is not the source J, it is $\bar{\phi}$. If one considers a theory with spontaneous symmetry breaking, then $\bar{\phi} \neq 0$ in the limit as J tends to zero. The correct Taylor expansion is obtained by shifting the field ϕ by an amount v where v is defined as

$$v = \lim_{J \to 0} \bar{\phi} \ . \tag{2.1.30}$$

Thus the new expression for the generating functional is given by

$$\Gamma(\bar{\phi}) = \sum_{n=0}^{\infty} \frac{1}{n!} \int \prod_{i=1}^{n} d^4x_i \Gamma^n(x_1, \cdots, x_n, v) \left(\bar{\phi}(x_1) - v\right) \cdots \left(\bar{\phi}(x_n) - v\right) \ . \tag{2.1.31}$$

Therefore to calculate the effective potential, or the n-point vertex functions, in a theory with spontaneous symmetry breaking, one should shift the fields in the symmetric theory by an amount v and use the shifted Lagrangian for perturbative calculations.

2.1.5. The Effective Potential at One-Loop Order.

In order to compute the effective potential by using Eq. (2.1.29), the n-point vertex functions evaluated at zero momentum are needed. The vertex functions can be computed by using the loop expansion, thus as a first approximation, one can consider the calculation of the effective potential at one-loop order. The Lagrangian density for a scalar field theory with a quartic interaction is given by

$$\mathcal{L} = -\frac{1}{2}\partial_\mu \phi(x)\,\partial^\mu \phi(x) - \frac{1}{2}m^2\phi^2(x) - \frac{1}{4!}g^2\phi^4(x) \tag{2.1.32}$$

where the tree-level contribution to the effective potential is

$$V^0_{eff}(v) = \frac{1}{2}m^2v^2 + \frac{g^2}{4!}v^4\,. \tag{2.1.33}$$

The Feynman graphs contributing to the effective potential at one-loop order are illustrated in Fig. 2.1.1.

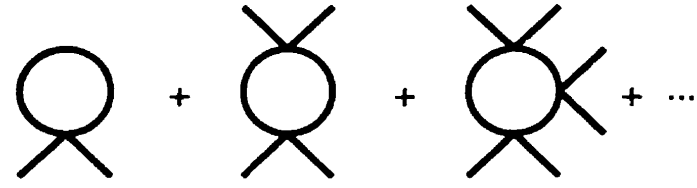

Figure 2.1.1: One-loop contributions to the effective potential.

Using the Feynman rules presented previously, it is not difficult to show that the one-loop contribution to the effective potential is given by

$$V^1_{eff}(v) = -\sum_{n=1}^{\infty}\frac{1}{2n}\left(\frac{-g^2v^2}{2}\right)^n \int \frac{d^4p}{(2\pi)^4}\frac{1}{(p^2+m^2)^n}\,. \tag{2.1.34}$$

After the sum over n is performed the following expression is obtained:

$$V^1_{eff}(v) = \frac{1}{2}\int \frac{d^4p}{(2\pi)^4}\log\left(p^2+m^2+\frac{g^2v^2}{2}\right)\,. \tag{2.1.35}$$

The effective potential accurate to one-loop order is given by the sum of the tree-level term and the one-loop term which is

$$V_{eff}(v) = V^0_{eff}(v) + V^1_{eff}(v) \tag{2.1.36}$$

where the tree-level term is given by Eq. (2.1.33).

To sum an infinite number of Feynman graphs beyond one-loop order becomes an impractical task if one continues to analyze the contributions on a diagram by diagram basis. It can be shown[28] that the effective potential can be evaluated in a much more efficient way by considering the shifted Lagrangian density. If one considers a theory described by the Lagrangian density $\mathcal{L}(\phi(x))$ and action S, then one can define a new Lagrangian density $\mathcal{L}_s(\phi(x), v)$ through the procedure

$$\int d^4x \mathcal{L}_s\left(\phi\left(x\right), v\right) = S\left[\phi\left(x\right) + v\right] - S\left[v\right] - \int d^4x \phi\left(x\right) \frac{\delta S\left[v\right]}{\delta v} \tag{2.1.37}$$

where the variable v is a position-independent shifting field. The second term on the right-hand side of Eq. (2.1.37) keeps the vacuum energy of the shifted theory at zero. The final term ensures that the tadpole contribution from shifting the Lagrangian density is also cancelled.

By using the shifted theory to define a new propagator $\mathcal{D}(p, v)$ and a set of new interaction vertices, the effective potential is found to be

$$V_{eff}\left(v\right) = V^0_{eff}\left(v\right) + \frac{1}{2} \int \frac{d^4p}{\left(2\pi\right)^4} \log\left(det\mathcal{D}^{-1}\left(p, v\right)\right) + \langle exp\left(\int d^4x \mathcal{L}_I\left(\phi\left(x\right), v\right)\right)\rangle \ . \tag{2.1.38}$$

The first term in Eq. (2.1.38) is simply the classical tree-level potential. The second term is the one-loop potential and is equivalent to Eq. (2.1.35) for the case of a single scalar field. The final term summarizes the following operations: Compute all the 1PI vacuum graphs using the Feynman rules of the shifted theory and delete the overall space-time volume factor of $\int d^4x$. The final term in Eq. (2.1.38) begins at two-loop order. Therefore, for most practical purposes, Eq. (2.1.38) is used to evaluate the effective potential within the loop expansion.

2.2. Quantum Field Theory at Finite Temperature

2.2.1. The Partition Function

From statistical mechanics it is known that the Grand-Canonical Partition Function is given by

$$\mathcal{Z} = Tr\ exp\left(-\beta\left(\mathcal{H} - \mu_i \mathcal{N}_i\right)\right) \tag{2.2.1}$$

where $\beta = 1/k_B T$, $\mathcal{H}$ is the Hamiltonian operator, μ_i is the set of chemical potentials and $\mathcal{N}_i$ is a set of conserved number operators. In a relativistic theory, the number of particles is not a conserved quantity, however, the difference between the number of particles and antiparticles of a particular species is conserved. From the Grand-Canonical Partition Function all standard thermodynamic properties of a system may be determined. For example, the pressure, particle number, entropy and internal energy are given by the following relations:

$$P = T\frac{\partial \log(\mathcal{Z})}{\partial V} \tag{2.2.2}$$

$$N_i = T\frac{\partial \log(\mathcal{Z})}{\partial \mu_i} \tag{2.2.3}$$

$$S = \frac{\partial (T \log(\mathcal{Z}))}{\partial T} \tag{2.2.4}$$

$$E = -PV + TS + \mu_i N_i \,. \tag{2.2.5}$$

Thus, to determine the properties of a particular system, the partition function must be evaluated.

A first step in attempting to evaluate $\mathcal{Z}$ is to rewrite the trace operation as an integral over all the states to obtain

$$\mathcal{Z} = \int d\phi_a \langle \phi_a | e^{(-\beta(\mathcal{H} - \mu_i \mathcal{N}_i))} | \phi_a \rangle \,. \tag{2.2.6}$$

One can now make use of the fact that the transition amplitude of going from one state to another is given by the path integral

$$\langle \phi_b | e^{-i\mathcal{H}(t_b - t_a)} | \phi_a \rangle = \int \mathcal{D}\pi \int \mathcal{D}\phi \; exp\left(i \int_{t_a}^{t_b} dt \int d^3x \left(\pi\dot{\phi} - \tilde{\mathcal{H}}(\pi, \phi) \right) \right) \tag{2.2.7}$$

where $\tilde{\mathcal{H}}$ is the classical Hamiltonian density. In order to evaluate the amplitude in Eq. (2.2.6), the field integration in Eq. (2.2.7) must be constrained such that $\phi_b(\mathbf{x}, t_b) = \phi_a(\mathbf{x}, t_a)$. Using this fact and letting $t_f = t_b - t_a$ allows one to rewrite Eq. (2.2.7) as

$$\langle \phi_a(t_f) | e^{-i\mathcal{H}t_f} | \phi_a(0) \rangle = \int \mathcal{D}\pi \int_{\phi_a(0)}^{\phi_a(t_f)} \mathcal{D}\phi \; exp\left(i \int_0^{t_f} dt \int d^3x \left(\pi\dot{\phi} - \tilde{\mathcal{H}}(\pi, \phi) \right) \right) \tag{2.2.8}$$

where $\phi_a(0) = \phi_a(\mathbf{x}, 0)$ and $\phi_a(t_f) = \phi_a(\mathbf{x}, t_f)$. One can now substitute Eq. (2.2.8) into Eq. (2.2.6) to obtain a path integral expression for the partition function $\mathcal{Z}$. To make this substitution, one can switch to imaginary time† and let the time integration range from 0 to $-i\beta$. After making a change of variable $it = \tau$, the following equation is obtained:

$$\mathcal{Z} = \int \mathcal{D}\pi \int_{periodic} \mathcal{D}\phi \, exp\left(\int_0^\beta d\tau \int d^3x \left(i\pi \frac{\partial \phi}{\partial \tau} - \tilde{\mathcal{H}}(\pi, \phi) + \mu \tilde{\mathcal{N}}(\pi, \phi)\right)\right) \quad (2.2.9)$$

where $\tilde{\mathcal{N}}(\pi, \phi)$ is the classical conserved charge density. The term "periodic" means that the field integration is constrained such that $\phi(\mathbf{x}, 0) = \phi(\mathbf{x}, \beta)$. This "periodic" boundary condition applies only to Bosons. It can be shown[22] that Fermions must obey "anti-periodic" boundary conditions where $\psi(\mathbf{x}, 0) = -\psi(\mathbf{x}, \beta)$. This difference is due to the fact that Bosons and Fermions obey different statistics. It should be noted that the conjugate momentum integration is unconstrained.

If one considers the case of a neutral-scalar field then the charge-density term in Eq. (2.2.9) will vanish. If $\tilde{\mathcal{H}}(\pi, \phi)$ is a quadratic function of the conjugate momentum π, then the momentum integration can be evaluated explicilty as a Gaussian integral. After performing the momentum integration, one obtains the simple expression

$$\mathcal{Z} = N \int_{periodic} \mathcal{D}\phi \, exp\left(\int_0^\beta d\tau \int d^3x \mathcal{L}(\phi, \partial\phi)\right) \quad (2.2.10)$$

where $\mathcal{L}(\phi, \partial\phi)$ is the classical Lagrangian density of the system under consideration and N is a normalization coefficient. The argument of the exponential in Eq. (2.2.10) is the classical action of the system and it may be represented by $\mathcal{S}$. Thus the partition function can be written in the very compact form:

$$\mathcal{Z} = N \int_{periodic} \mathcal{D}\phi \, exp(\mathcal{S}) \; . \quad (2.2.11)$$

† This convention of switching to imaginary time is known as the Imaginary-Time Formalism and was developed by Matsubara[29]. One can also choose to evaluate the partition function in real time, however, for our purposes it is convenient to use the Imaginary-Time Formalism. For more information on the Real-Time Formalism the reader is encouraged to read the excellent review paper by Landsman and van Weert[30].

If one adds a source term to the action in Eq. (2.2.11), then one regains the generating functional given by Eq. (2.1.2). This is a particularly interesting fact for it allows one to interpret the generating functional and the partition function as being essentially the same object. Finite-temperature Green's functions can be calculated using an approach similar to that used for zero-temperature Green's functions. The Feynman rules for the finite-temperature Green's functions are discussed in the next subsection.

2.2.2. The Finite-Temperature Feynman Rules

The Feynman rules for calculating graphs in finite-temperature field theories are identical to the rules given for zero-temperature theories in all but one respect. As already explained, at finite-temperature, the fields are constrained such that Bosonic fields are periodic in imaginary-time and the Fermionic fields are anti-periodic in imaginary-time. Given these facts implies that the Fourier transform of the Bosonic field $\phi(x,\tau)$ can be expressed as

$$\phi\left(\mathbf{x},\tau\right)=\left(\frac{V}{\beta}\right)^{1/2}\sum_{n=-\infty}^{\infty}\int\frac{d^{3}\mathbf{p}}{(2\pi)}e^{i(\mathbf{p}\cdot\mathbf{x}+\omega_{n}\tau)}\phi\left(\omega_{n},\mathbf{p}\right) \tag{2.2.12}$$

where $\omega_n = 2\pi nT$ where n is an integer and V is the volume. Notice that this ensures that $\phi(\mathbf{x},0) = \phi(\mathbf{x},\beta)$ for all $\mathbf{x}$. In the case of Fermions, the discrete energies are constrained such that $\omega_n = (2n+1)\pi T$ with n an integer. This ensures that the Fermionic fields satisfy the boundary condition that $\psi(\mathbf{x},0) = -\psi(\mathbf{x},\beta)$ for all $\mathbf{x}$.

To account for these different boundary conditions, the factor of

$$\int\frac{d^{4}k_{j}}{(2\pi)^{4}}$$

that is included for each independent momenta k_j is replaced with the factor

$$T\sum_{n}\int\frac{d^{3}\mathbf{k}_{j}}{(2\pi)^{3}}\,.$$

The loop integrations associated with zero-temperature field theory are replaced with what are known as Matsubara sums. The Matsubara sum includes a sum over the discrete energies and an integration over the three-momenta. Methods for evaluating such sums can be found in the literature[31].

2.2.3. The Helmholtz Free Energy

One notices in Eq. (2.2.2) through Eq. (2.2.5) that the logarithm of the partition function plays an essential role, thus we shall turn our attention to this quantity. The grand partition function is related to the Helmholtz free energy $\mathcal{A}$ through the relation

$$\log \mathcal{Z} = -\beta \mathcal{A} \,, \tag{2.2.13}$$

where the Helmholtz free energy or "grand potential" is proportional to the volume of the system. Thus $\mathcal{A}$ is an extensive quantity from which intensive quantities such as the pressure P may be determined;

$$P = -\left(\frac{\partial \mathcal{A}}{\partial V}\right)_{T,N_i} \,. \tag{2.2.14}$$

Before taking the logarithm of the partition function, it is useful to expand it in the following way.

The action $\mathcal{S}$ can be expressed as the sum of two contributions

$$\mathcal{S} = \mathcal{S}_0 + \mathcal{S}_I \,. \tag{2.2.15}$$

The first term, $\mathcal{S}_0$, is the contribution to the total action from the free part of the Lagrangian. The second term, $\mathcal{S}_I$, represents the contributions from the interaction part of the Lagrangian. If one assumes that that $\mathcal{S}_0 \gg \mathcal{S}_I$ then Eq. (2.2.11) can be expanded in powers of $\mathcal{S}_I$ as follows;

$$\mathcal{Z} = N \int_{periodic} \mathcal{D}\phi \, e^{\mathcal{S}_0} \sum_{i=0}^{\infty} \frac{1}{i!} \mathcal{S}_I^i \tag{2.2.16}$$

where we have have used the fact that

$$e^x = \sum_{i=0}^{\infty} \frac{x^i}{i!} \,. \tag{2.2.17}$$

Taking the logarithm of Eq. (2.2.16) one obtains

$$\log \mathcal{Z} = \log \left(N \int \mathcal{D}\phi \, e^{\mathcal{S}_0} \right) + \log \left(1 + \frac{\sum_{i=1}^{\infty} \frac{1}{i!} \int \mathcal{D}\phi \, \mathcal{S}_I^i e^{\mathcal{S}_0}}{\int \mathcal{D}\phi \, e^{\mathcal{S}_0}} \right) \tag{2.2.18}$$

or

$$\log \mathcal{Z} = \log \mathcal{Z}_0 + \log \mathcal{Z}_I \tag{2.2.19}$$

which explicitly separates the contributions to $\log \mathcal{Z}$ into two distinct pieces. The first term represents the "noninteracting" or "ideal-gas" contribution, whereas the second term represents the interaction contribution. The ideal-gas contribution is easily evaluated[27] and found to be

$$\log \mathcal{Z}_0 = \mp V \int \frac{d^3p}{(2\pi)^3} \log\left(1 \mp e^{-\beta\omega}\right) \tag{2.2.20}$$

where $\omega = \sqrt{p^2 + m^2}$. The upper sign is for a noninteracting gas of Bosons and the lower sign is for a noninteracting gas of Fermions.

The quantities that require more effort to compute appear in $\log \mathcal{Z}_I$ and are of the form

$$\langle \mathcal{S}_I^i \rangle = \frac{\int \mathcal{D}\phi \, \mathcal{S}_I^i e^{\mathcal{S}_0}}{\int \mathcal{D}\phi \, e^{\mathcal{S}_0}} \tag{2.2.21}$$

where the field integration is constrained by the appropriate boundary conditions. The terms in Eq. (2.2.21) can be represented by Feynman diagrams and evaluated using the finite-temperature Feynman rules. As an example, the two and three loop contributions to the free energy of a scalar theory with a quartic interaction are displayed in Fig. 2.2.1. Only the connected graphs contribute to the free energy of the system. This is not a surprising fact given that the generating functional for the connected graphs $\mathcal{W}$ is given by the logarithm of the generating functional $\mathcal{Z}$. A short proof that $\log \mathcal{Z}_I$ consists of a sum of connected diagrams is as follows.

Figure 2.2.1: Diagrams contributing to the free energy.

From Eq. (2.2.16) it follows that $\mathcal{Z}_I$ can be written in the folowing way

$$\mathcal{Z}_I = \sum_{i=0}^{\infty} \frac{1}{i!} \langle \mathcal{S}_I^i \rangle \, . \tag{2.2.22}$$

In general $\langle S_I^i \rangle$ can be written as a sum of terms each of which is a product of connected diagrams.

$$\langle S_I^i \rangle = \sum_{a_1=0,\cdots,a_i=0}^{\infty} \frac{i!}{a_1! \cdots a_i!} \langle S_I^1 \rangle_c^{a_1} \langle S_I^2 \rangle_c^{a_2} \cdots \langle S_I^i \rangle_c^{a_i} \delta_{a_1+2a_2+\cdots+ia_i,i} \tag{2.2.23}$$

The combinatoric factors account for the indistinguishability of diagrams and the Kronecker delta function picks out contributions of a similar order. By substituting Eq. (2.2.23) into Eq. (2.2.22) the delta function is eliminated by the sum over i and one is left with the expression

$$\mathcal{Z}_I = \sum_{a_1=0,a_2=0,a_3=0,\cdots}^{\infty} \frac{\langle S_I^1 \rangle_c^{a_1}}{a_1!} \frac{\langle S_I^2 \rangle_c^{a_2}}{a_2!} \frac{\langle S_I^3 \rangle_c^{a_3}}{a_3!} \cdots \tag{2.2.24}$$

which is equivalent to

$$\mathcal{Z}_I = exp\left(\sum_{n=0}^{\infty} \langle S_I^n \rangle_c \right) . \tag{2.2.25}$$

From Eq. (2.2.25) it follows that $\log \mathcal{Z}_I$ is given by the sum over connected diagrams. The partition function has been evaluated to high orders in both QED and QCD and the results can be found in the papers by Baluni[32] and Freedman and McLerran[33].

2.2.4. High-Temperature Symmetry Restoration and the Effective Potential

It has already been established in section (2.1.4), that the ground state of a system can be determined by studying the effective potential $V_{eff}(v)$. It is natural to ask whether symmetries that are broken at zero temperature can be restored by heating the system to sufficiently high temperatures. If we consider the effective potential to be a function of both the expectation value of $\phi(x)$, which is given by v, and the temperature T, then this question can be answered by finding the minima of $V_{eff}(v,T)$. At temperatures $T < T_c$, where T_c is the critical temperature, the effective potential has a minimum at some finite value of $v \neq 0$. At temperatures $T > T_c$ the minimum occurs at $v = 0$ which signals the restoration of the symmetry. If there exists only one minimum at $T = T_c$, then the phase transition is second order. Systems which exhibit degenerate minima at $T = T_c$ are said to undergo first-order phase transitions.

To give an example, consider a hot scalar theory with spontaneous symmetry breaking due to a negative mass-squared term. The reason why the symmetry is restored is that the tree-level mass squared term receives a positive correction proportional to g^2T^2 at one-loop order. At low temperatures, $T < T_c$, the effective mass squared is dominated by the tree-level contribution and therefore remains negative signaling the broken-symmetry phase. At very high temperatures, $T > T_c$, the loop correction dominates and the effective mass squared is positive. The positive mass-squared term signals the restoration of the symmetry. A useful method for calculating the effective potential within perturbation theory is an effective-Lagrangian approach.

The problem with the standard perturbative expansion is that the wrong effective degrees of freedom are being used[34]. At energies of the order of the critical temperature, the temperature-dependent loop corrections to the mass of the scalar particles are of the same order as the tree-level mass. This is due to the fact that the one-loop mass correction receives considerable contributions over the complete range of integration. This implies that the high-energy degrees of freedom are as important as the low-energy degrees of freedom. By using the approach of Wilson[35–37], one can rearrange the Lagrangian such that the effective degrees of freedom implied by the tree-level terms are, in fact, the relevant degrees of freedom. Thus, if one computes the one-loop mass correction with the effective theory, one finds that the corrections are suppressed by powers of the coupling constant and that the integration receives contributions only over the relevant energy range, the one at which we are probing the physics.

It must be emphasized that we are not solving the famous problem of critical behaviour in three dimensions using perturbation theory. The problem in studying critical behaviour in three dimensions is that the vanishing renormalized mass invalidates the use of perturbation theory. In our problem the tree-level bare mass of the theory is zero and the renormalized mass is finite. The effective field theory approach allows one to take the theory with zero bare mass and derive a physically equivalent theory with a finite bare mass. It is the introduction of the finite bare

mass which restores perturbation theory. This effective-Lagrangian approach will be reviewed in the next chapter.

Chapter 3.
The Effective Lagrangian and the Renormalization Group

In this chapter, a scalar field theory with a momentum cutoff is reviewed. This model is used to introduce the essential concepts concerning effective Lagrangians and the renormalization group. The ideas presented will be used in subsequent chapters.

3.1. Scalar Field Theory with a Momentum Cutoff

In order to evaluate quantum corrections in perturbation theory, a regularization scheme is needed to deal with the ultraviolet divergences encountered in explicit calculations. For this study, a momentum-space cutoff is used to regularize the theory. The scale of the cutoff is chosen to be much greater than the scale of the physics which we are interested in probing. Physical quantities cannot depend on the value of the momentum cutoff because the cutoff is simply the mathematical device chosen to regularize the theory. One can choose a different regularization scheme, such as dimensional regularization[38], however, the physical predictions of the theory will be identical using either scheme.

To compensate for the cutoff dependence generated by the momentum cutoff, cutoff-dependent counterterms are added to the original Lagrangian. The counterterms ensure that all physical quantities calculated to a particular order in perturbation theory will remain independent of the cutoff. If the theory is renormalizable, it can be shown that only a finite number of counterterms are needed[39-40]. Since the physical predictions of the theory will be independent of the cutoff scale, one can assume that the cutoff scale is taken to infinity. The Lagrangian that is used for computing physical quantities, the bare Lagrangian, is given by

$$L = L_0 + L_{int} \tag{3.1.1}$$

where

$$L_0 = \int d^4p \left(-\frac{1}{2}\phi(p)\,\phi(-p)\,(p^2+m^2)\,K^{-1}\left(p^2/\Lambda^2\right)\right) \tag{3.1.2}$$

with

$$m^2 < \Lambda^2 \tag{3.1.3}$$

and

$$L_{int} = \int d^4x \left(-\frac{1}{2} A \partial_\mu \phi(x) \partial^\mu \phi(x) - \frac{1}{2} \delta m^2 \phi^2(x) - \frac{1}{4!} g^2 (1+B) \phi^4(x) \right) . \tag{3.1.4}$$

The free Lagrangian L_0 is written in momentum space to emphasize the fact that the propagator of the theory includes a cutoff function $K(p^2/\Lambda^2)$. The functional form of the cutoff function is not important[41]; all that is required is that it have the value 1 for $p^2 < \Lambda^2$ and vanish rapidly for values of $p^2 > \Lambda^2$. The cutoff-dependent parameter A is related to the wavefunction renormalization factor Z_ϕ through the equation

$$Z_\phi = 1 + A . \tag{3.1.5}$$

The parameter δm^2 represents the mass counterterm which is also cutoff dependent. Finally, B is the coupling-constant counterterm which also has Λ dependence. The generating functional for the n-point Green's functions is given by

$$\mathcal{Z}(J) = \int \mathcal{D}\phi \, exp \{ L_0 + \int d^4p J(p) \phi(-p) + L_{int} \} \tag{3.1.6}$$

where $J(p) = 0$ for $p^2 > \Lambda^2$. This last constraint ensures that one cannot probe the physics above the cutoff scale.

3.2. Integrating Over The High-Frequency Modes

To remove the high-frequency components of the field ϕ, all that is required is that the cutoff scale Λ be lowered. By lowering the cutoff scale to some finite value Λ, one has integrated out all modes from Λ to infinity. Since the cutoff scale is arbitrary, a change in the value of Λ should not change the physical predictions of the theory. Therefore, as one removes modes, new effective interactions are generated to compensate for the contributions of modes that have been integrated out. To illustrate this point, consider the generating functional for the scalar field:

$$\mathcal{Z}(J) = \int \mathcal{D}\phi \, exp \{ L_0(\phi, \Lambda) + \int d^4p J(p) \phi(-p) + L_{int}(\phi, \Lambda) \} \tag{3.2.1}$$

or

$$\mathcal{Z}(J) = \int \mathcal{D}\phi exp\left(\mathcal{S}(\phi)\right) . \tag{3.2.2}$$

The Λ dependence of L_0 is due to the cutoff function K and the cutoff dependence of L_{int} resides in the counterterms. Taking the derivative of Eq. (3.2.1) with respect to Λ yields

$$\frac{d\mathcal{Z}}{d\Lambda} = \int \mathcal{D}\phi\{\int d^4p \left(-\frac{1}{2}\phi(p)\,\phi(-p)\left(p^2+m^2\right)\frac{\partial K^{-1}}{\partial \Lambda}\right) + \frac{\partial L_{int}}{\partial \Lambda}\} exp\left(\mathcal{S}(\phi)\right) . \tag{3.2.3}$$

In order for the n-point vertex functions to remain unchanged as the cutoff is lowered, the derivative of $\mathcal{Z}$ with respect to Λ must be equal to zero. Therefore, the question that needs to be addressed is how must $\frac{\partial L_{int}}{\partial \Lambda}$ be chosen to compensate for the removal of modes.

As Λ is lowered, the propagation of modes with momentum $p^2 > \Lambda^2$ is damped by the cutoff function. Therefore, if one calculates the mass correction to some order in the loop expansion, there will be fewer momentum modes propagating through the internal lines in the theory with the lower cutoff . To compensate for this, the mass counterterm, found in L_{int}, should include the contribution of the modes that have been integrated out[42]. A similar argument can be used to account for the changes to the parameters A and B found in L_{int}. Along with the changes already described, new effective interactions of a different form are also needed. To see the need for these new interactions consider the scattering process represented by the Feynman diagram in Fig. 3.2.1.

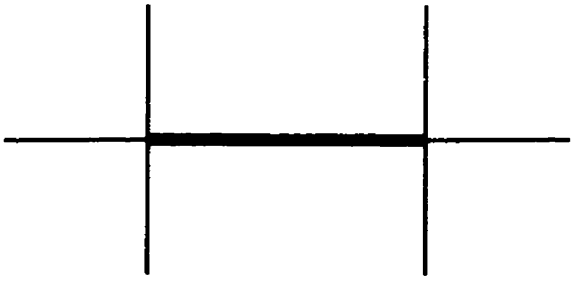

Figure 3.2.1: Scattering diagram in ϕ^4 theory.

As the cutoff Λ is reduced, fewer high-frequency modes can propagate along the internal line shown in bold. Thus the amplitude for this scattering process will differ from that computed in the theory with the higher cutoff. To make the amplitudes equal at $\mathcal{O}(g^4)$, an effective six-point interaction is needed in the theory with the lower cutoff. As one computes processes to higher orders in the coupling constant, a greater number of new effective interactions will be needed to compensate for the removal of the high-frequency modes. It can be shown[43] that as the cutoff Λ is reduced, the Lagrangian should be changed according to the following equation:

$$\begin{aligned}\frac{\partial L_{int}}{\partial \Lambda} = \int d^4p \left(-\frac{1}{2}\phi(p)\,\phi(-p)\left(p^2+m^2\right)^{-1}\frac{\partial K}{\partial \Lambda}\right) \\ \times\left(\frac{\delta L_{int}}{\delta\phi(-p)}\frac{\delta L_{int}}{\delta\phi(p)}+\frac{\delta^2 L_{int}}{\delta\phi(-p)\,\delta\phi(p)}\right)\end{aligned} \tag{3.2.4}$$

in order for the generating functional $\mathcal{Z}$ to remain unchanged. To see that this is in fact the case, simply substitute Eq. (3.2.4) into Eq. (3.2.3). It is easy to verify, after some mathematical manipulation, that one obtains

$$\frac{d\mathcal{Z}}{d\Lambda} = \int d^4p \frac{\partial K}{\partial \Lambda}\int \mathcal{D}\phi \frac{\delta}{\delta\phi(p)}\left(\left(\phi(p)\,K^{-1}+\frac{1}{2}\left(p^2+m^2\right)^{-1}\frac{\delta}{\delta\phi(-p)}\right)exp\left(\mathcal{S}\right)\right) \tag{3.2.5}$$

from which it follows that

$$\frac{d\mathcal{Z}}{d\Lambda} = 0\,. \tag{3.2.6}$$

Eq. (3.2.5) is equal to zero because $\frac{\partial K}{\partial \Lambda}$ vanishes for all momenta with $p^2 < \Lambda^2$. Recall that the source J also vanishes for all momenta with $p^2 > \Lambda^2$. Thus $\mathcal{Z}(J)$ and its functional derivatives, the n-point Green's functions, remain unchanged if the cutoff Λ is lowered and the Lagrangian is changed according to Eq. (3.2.4).

An interesting feature of Eq. (3.2.4) is that it has a simple graphical interpretation. As already stated, when the cutoff is lowered compensating terms must be added to the Lagrangian. The first term in Eq. (3.2.4) represents graphs where the differentiated propagator connects two vertices, whereas the second term is described by graphs in which the propagator connects to a single vertex. Examples of these graphs are shown in Fig. 3.2.2.

Figure (a) represents the effective six-point interaction created by connecting two four-point vertices with the differentiated propagator. This contribution arises

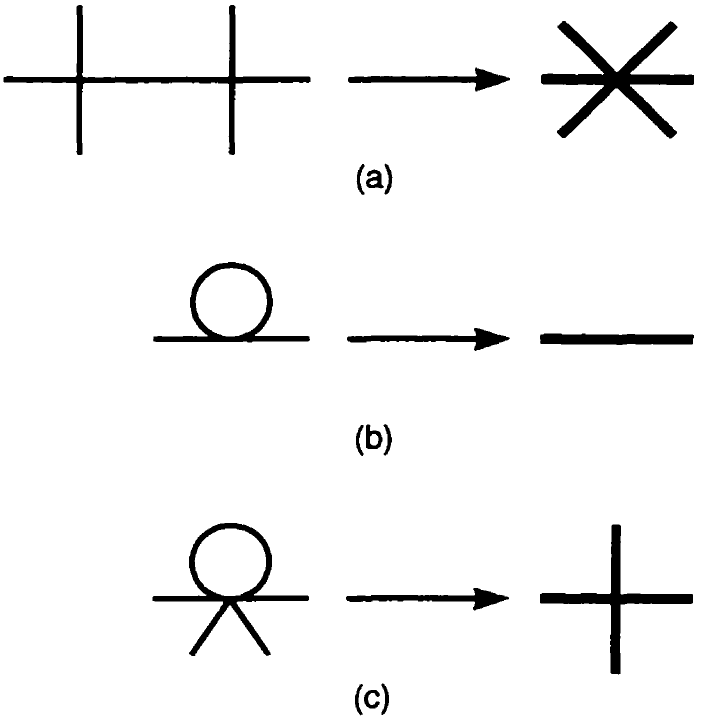

Figure 3.2.2: Graphical Interpretation of the Effective Interactions.

at $\mathcal{O}(g^4)$. Figure (b) represents the correction to the two-point function created by connecting the differentiated propagator to the four-point vertex. This correction is of $\mathcal{O}(g^2)$. Finally, in figure (c), the differentiated propagator is connected to the effective six-point interaction, which in turn creates a correction to the four-point vertex at $\mathcal{O}(g^4)$. In this manner, an infinite number of effective interactions are created in a self-consistent fashion to ensure that the effective Lagrangian with the lower cutoff scale describes the same physics as the original Lagrangian.

3.3. The Renormalization-Group Equation

The bare Lagrangian is the Lagrangian that yields finite physical quantities to any desired order. One can rewrite the bare Lagrangian given by Eq. (3.1.1) as

$$L = -\frac{1}{2}\partial_\mu \phi_B \partial^\mu \phi_B - \frac{1}{2} m^2_{B(m,g,\Lambda)} \phi^2_B - \frac{1}{4!} g^2_{B(g,m,\Lambda)} \phi^4_B \qquad (3.3.1)$$

where it is understood that all propagators are cutoff at the scale Λ. The quantities ϕ_B, $m_{B(m,g,\Lambda)}$ and $g^2_{B(g,m,\Lambda)}$ are known as the bare field, the bare mass, and the bare

coupling constant respectively. These quantities are related to the renormalized field ϕ, the renormalized mass m, and renormalized coupling constant g^2 through the following equations:

$$\begin{aligned} \phi_B &= \sqrt{Z_{\phi(m,g,\Lambda)}}\phi \\ m^2_{B(m,g,\Lambda)} &= \frac{m^2+\delta m^2}{Z_{\phi(m,g,\Lambda)}} \\ g^2_{B(g,m,\Lambda)} &= \frac{g^2\,(1+B)}{Z^2_{\phi(m,g,\Lambda)}} \\ Z_{\phi(m,g,\Lambda)} &= 1+A\,. \end{aligned} \tag{3.3.2}$$

These bare parameters can be calculated perturbatively and expressed as functions of the finite physical quantities m and g. The functions $Z_{\phi(m,g,\Lambda)}$, $m^2_{B(m,g,\Lambda)}$ and $g^2_{B(g,m,\Lambda)}$ diverge in the limit as Λ tends to infinity, however, all the n-point functions computed to a given order in g, using the bare Lagrangian, are finite and independent of Λ.

The fact that all renormalized quantities are independent of Λ can be summarized in the following differential equation:

$$\Lambda\frac{d}{d\Lambda}\Gamma^n_R\,(m,g,p_i) = 0\,. \tag{3.3.3}$$

In Eq. (3.3.3), $\Gamma^n_R(m,g,p_i)$ represents a general renormalized n-point vertex function which is a function of the renormalized mass m, the renormalized coupling constant g^2, and external momenta p_i. The renormalized vertex functions can be expressed in terms of the bare vertex functions as

$$\Gamma^n_R\,(m,g,p_i) = Z^{n/2}_\phi(m,g,\Lambda)\Gamma^n_B\left(m_B,g^2_B,\Lambda,p_i\right) \tag{3.3.4}$$

from which it follows that

$$\Lambda\frac{d}{d\Lambda}\left(Z^{n/2}_\phi(m,g,\Lambda)\Gamma^n_B\left(m_B,g^2_B,\Lambda,p_i\right)\right) = 0\,. \tag{3.3.5}$$

By taking the derivative in Eq. (3.3.5) with m and g held fixed, one obtains the following partial-differential equation:

$$\left[\frac{n}{2}\gamma_\phi + \Lambda\frac{\partial}{\partial\Lambda} + \beta\frac{\partial}{\partial g^2_B} + m_B\gamma_m\frac{\partial}{\partial m_B}\right]\Gamma^n_B\left(m_B,g^2_B,\Lambda,p_i\right) = 0\,, \tag{3.3.6}$$

which is the renormalization-group equation for the bare theory with the functions γ_ϕ, β, and γ_m defined by

$$\begin{aligned} \gamma_\phi &= \Lambda \left(\frac{\partial \log Z_\phi}{\partial \Lambda} \right) \\ \beta &= \Lambda \left(\frac{\partial g_B^2}{\partial \Lambda} \right) \\ m_B \gamma_m &= \Lambda \left(\frac{\partial m_B}{\partial \Lambda} \right) . \end{aligned} \tag{3.3.7}$$

The importance of Eq. (3.3.6) is that it describes how the bare n-point vertex functions, the bare mass, the bare coupling constant, and the bare field normalization must vary with a change in the cutoff Λ in order to preserve the renormalization conditions. The renormalization conditions may be summarized as follows:

$$\begin{aligned} \Gamma_R^2(m, g, 0) &= -m^2 \\ \frac{\partial}{\partial k^2} \Gamma_R^2(m, g, k) &= -1 \\ \Gamma_R^4(m, g, 0) &= -g^2 . \end{aligned} \tag{3.3.8}$$

In this chapter we have reviewed the construction of the bare Lagrangian and the regularization of the theory by use of a momentum cutoff. The renormalization-group equation that is satisfied by both the bare and renormalized vertex functions is also given. We have also described how an effective Lagrangian may be created by lowering the momentum-cutoff scale and that new effective interactions are generated as the cutoff scale is changed. As already discussed, an infinite number of effective interactions are generated as the cutoff scale is lowered. In order to have a consistent perturbative expansion in the effective theory, one must be able to estimate the relative sizes of the effective interactions so that the effective theory can be truncated to any given order in the coupling-constant expansion. A method by which the strengths of these new interactions can be estimated is presented in the next chapter.

Chapter 4.
Estimating the Strengths of Effective Interactions

A method for estimating the strengths of the effective-interactions is reviewed in this chapter. Simple power-counting arguments are used to determine the order at which contact and derivative interactions contribute.

4.1. Contact Interactions

The first type of interaction that will be studied is the contact or nonderivative interaction. These interactions have a very simple general form. They can be represented by a number, the strength of the coupling, multiplied by powers of the field ϕ. For example, consider the massive scalar-field theory with a quartic coupling presented in the previous chapter. If one decides to lower the cutoff Λ to some finite value, which is equivalent to integrating over all modes with momenta greater than the cutoff, then one will obtain an infinite number of effective contact interactions of the form

$$C_n\left(m, g, \Lambda, T\right) \phi^n\left(x\right)$$

where n is an even number. The coefficient function is considered to be a function of the renormalized mass, the renormalized coupling, the cutoff, and the temperature of the system since we are interested in the case of a scalar field at finite temperature. The coefficient functions play the same role as the bare parameters of the theory. What is required is a general method for estimating the size of $C_n(m, g, \Lambda, T)$ so that the effective Lagrangian may be truncated at a particular order in the coupling constant.

The behaviour of the coefficient functions may be determined by considering an L-loop calculation of a vertex function with n external lines. Since the original theory involved only a quartic interaction, we need only consider graphs constructed from four-point vertices. The generic behaviour of a graph constructed from V vertices at L-loop order is given by

$$C_n\left(m, g, \Lambda, T\right) \approx g^{2V} \left(T \int_{\Lambda} d^3\mathbf{k}\right)^L \left(\frac{1}{k^2 + m^2}\right)^P . \qquad (4.1.1)$$

There is a factor of g^2 for every vertex and a factor of $(k^2 + m^2)^{-1}$ for every propagator. For every loop there is a thermal sum to be performed, however, since we are interested in calculating the most infrared-singular contributions of the coefficient functions, only the infrared behaviour needs to be studied. To achieve this, the cutoff will be chosen such that $\Lambda < T$. This choice of cutoff implies that only the $n = 0$ term in the Matsubara sum needs to be considered. The lower limit of the three-momentum integration is also cutoff at Λ to ensure only momenta above the cutoff are integrated over. If the cutoff is chosen such that $\Lambda > m$, then the mass can be neglected and the leading infrared behaviour will be given by the cutoff Λ.

The next step is to rewrite the right-hand side of Eq. (4.1.1) in terms of the number of external lines n and the number of loops L. Using the "conservation of ends" one can make the substitution

$$P = 2V - \frac{n}{2} . \tag{4.1.2}$$

One can also use the fact that the number of internal lines minus the number of momentum constraints gives the number of independent momenta or loops:

$$P - (V - 1) = L . \tag{4.1.3}$$

Incorporating the above relationships and estimating the integral on dimensional grounds yields

$$C_n (g, \Lambda, T) \approx g^{n-2} \Lambda^{4-n} \left(\frac{g^2 T}{\Lambda} \right)^L . \tag{4.1.4}$$

Thus the generic behaviour of an L-loop vertex with n external legs is given by Eq. (4.1.4). Notice that the coefficient goes like a power of $1/\Lambda$, and that this power becomes more severe at higher orders in the loop expansion. Clearly, if $\Lambda \sim \mathcal{O}(g^2 T)$ then higher terms in the loop expansion are not suppressed by the small coupling g. It should be stressed that this estimate applies to the infrared behaviour that arises when all L of the loop momenta approach Λ together.

Even more dangerous possibilities arise from "ring" graphs, such as the one shown in Fig. 4.1.1, which involve many self-energy insertions along a single, $n = 0$ Matsubara frequency, line. In graphs like this, each propagator introduces an

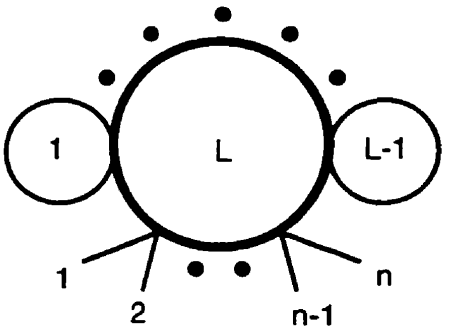

Figure 4.1.1: L-loop ring diagram with n external lines.

additional factor of $1/k^2$, while there is only a single factor of $d^3\mathbf{k}$ for the entire line. As a result these graphs can diverge more severely, with successive loops diverging with an additional factor of T/Λ in addition to those of Eq. (4.1.4). It is easy to show that the infrared behaviour of these "ring" graphs is described by

$$C_n\left(g,\Lambda,T\right) \approx \frac{g^{n-2}\Lambda^{5-n}}{T}\left(\frac{g^2T^2}{\Lambda^2}\right)^L \tag{4.1.5}$$

where $L \geq 2$. The loop expansion therefore breaks down for infrared cutoffs with $\Lambda \sim \mathcal{O}(gT)$. To maintain perturbative calculability, the cutoff must be chosen such that $\Lambda \gg \mathcal{O}(gT)$. If $\Lambda \sim \mathcal{O}(gT)$ then the series in g is not the loop expansion unlike the zero-temperature case.

Eq. (4.1.5) can be used to estimate the strengths of the effective contact interactions. For example, to determine which interactions have coefficients of $\mathcal{O}(g^2)$, then from Eq. (4.1.5) with $\Lambda \gg \mathcal{O}(gT)$, it is easy to see that there are only two possibilities. There is the one-loop correction to the two-point function ($n = 2, L = 1$) and there is the tree-level contribution to the four-point function ($n = 4, L = 0$). Therefore, if one needs to obtain the effective Lagrangian to $\mathcal{O}(g^2)$, all that is needed is that the high-frequency modes be integrated over at one-loop order in the two-point function. This analysis can be extended to $\mathcal{O}(g^4)$ without much difficulty. From Eq. (4.1.5) one finds that there now exist three new possibilities. There are two-loop corrections to the two-point function ($n = 2, L = 2$), there is a one-loop

correction to the four-point function ($n = 4, L = 1$), and finally there is a new effective six-point contact interaction ($n = 6, L = 0$). Thus, to obtain the effective Lagrangian to $\mathcal{O}(g^4)$, one must make the following changes: Integrate over the high-energy modes in the two-point function at both one and two-loop order. Integrate out high-frequency modes in the four-point function at one-loop order. Add a six-point contact interaction[42] with a coefficient of $\mathcal{O}(g^4)$ chosen such that the original theory and effective theory agree on all estimates of physical processes at $\mathcal{O}(g^4)$. Continuing in this manner, one can include all the non-derivative interactions to any order in the coupling g.

4.2. Derivative Interactions

It is essential, if we wish to have a consistent perturbative expansion, to estimate the strengths of the derivative interactions that appear in the effective Lagrangian. This can be achieved by considering the solution to the classical equation of motion of the field ϕ. The reason why solutions to the lowest-order equations of motion can be used to simplify higher-order terms in the effective-Lagrangian is that this is equivalent to performing a field redefinition[44]. The effective theory is simplified at $\mathcal{O}(g^n)$ and the effect of the field redifinition appears at $\mathcal{O}(g^{n+2})$ and greater. The physics of the theory is not altered by the field redefintion. Any derivative interaction that cannot be reexpressed as higher-order interactions must be kept within the effective theory.

The classical equation of motion of the field is given by the Euler-Lagrange equation which is

$$\Box\, \phi + P'(\phi) = 0\,. \tag{4.2.1}$$

For a free scalar field this is simply the Klein-Gordon equation. The function $P(\phi)$ represents the potential of the effective theory, and to lowest order in g is given by

$$P(\phi) = \frac{1}{2} m_{B(m,g,\Lambda)}^2 \phi^2 + \frac{1}{4!} g^2 \phi^4 + \mathcal{O}\left(g^4\right) \tag{4.2.2}$$

where $m_{B(m,g,\Lambda)}^2$ is the square of the effective mass. To simplify matters, we will assume that the original Lagrangian was that of a massless scalar field so that

$m = 0$. It will be shown in the next chapter that to lowest order $m_B^2(g,\Lambda) \sim \mathcal{O}(g^2T^2)$. Therefore, the behaviour of the lowest-order solution is

$$\Box\ \phi \sim \mathcal{O}\left(g^2T^2\right)\phi + \mathcal{O}\left(g^2\right)\phi^3 + \mathcal{O}\left(g^4\right)\ . \tag{4.2.3}$$

One can now use Eq. (4.2.3) to determine the strengths of the derivative interactions.

All terms in the effective theory must have an even dimension. This is due to the fact that each term consists of a product of an even number of fields ϕ, and that the derivative operators must act in pairs. Thus one can classify the derivative interactions by their dimensions. For example, a dimension-four derivative interaction must consist of two powers of the field ϕ and two derivative operators. These terms represent momentum-dependent corrections to the two-point function and first appear at $\mathcal{O}(g^4)$. The two possibilities are $\partial_\mu\phi\partial^\mu\phi$ and $\phi\ \Box\ \phi$. Since terms which are total derivatives do not contribute to the action of the theory, then it follows that $\partial_\mu\phi\partial^\mu\phi$ term can always be written as a $\phi\ \Box\ \phi$ term. By using the lowest-order solution to the equation of motion this can be replaced by contact interactions whose coupling is of $\mathcal{O}(g^2)$ higher. Therefore, these corrections contribute to $\mathcal{O}(g^6)$ and may be neglected.

As a second example, consider dimension-six terms in the effective theory. There exist two possibilities. There are terms that have four powers of the field ϕ and two derivatives and there are terms with two powers of the field and four derivatives. First consider the terms with two derivatives such as $\phi^3\ \Box\ \phi$ and $\phi^2\partial_\mu\phi\,\partial^\mu\phi$. These terms represent momentum-dependent corrections to the four-point function and first appear at one-loop and contribute to $\mathcal{O}(g^4)$. The Feynman graphs for these corrections are given in Fig. 4.2.1. Once again, using the fact that terms that are total derivatives do not contribute to the action, we obtain

$$0 = \int d^4x\ O\left(g^4\right)\partial_\mu\left(\phi^3\partial^\mu\phi\right) = \int d^4x\ O\left(g^4\right)\left[3\phi^2\partial_\mu\phi\,\partial^\mu\phi + \phi^3\ \Box\ \phi\right] \tag{4.2.4}$$

which indicates that the dimension-six interactions with two derivatives can be represented by the $\phi^3\ \Box\ \phi$ term. By substituting the lowest-order solution to the classical equation of motion into $\phi^3\ \Box\ \phi$, one finds that the derivative-interaction term may be replaced by non-derivative interactions that are of higher-order in the

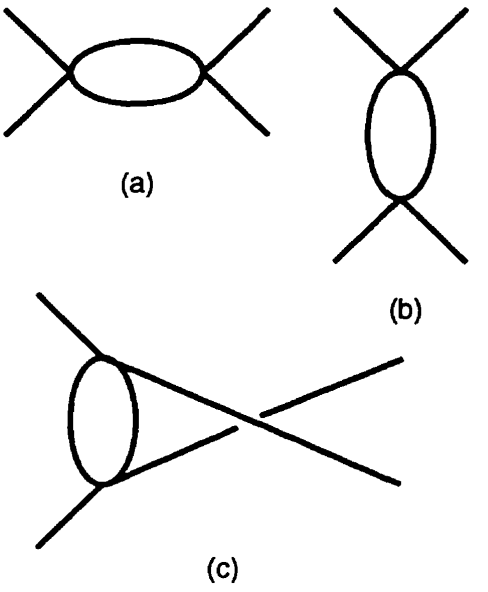

Figure 4.2.1: 1-loop corrections to the four-point function.

coupling constant:

$$\int d^4x \; O\left(g^4\right)\left[\phi^3 \; \Box \; \phi\right] \sim \int d^4x \; O\left(g^6\right)\left[\phi^4 T^2\right] + \int d^4x \; O\left(g^6\right)\left[\phi^6\right]. \qquad (4.2.5)$$

Using a similar analysis, it is easy to show that the terms with four derivatives and two powers of the field contribute to $\mathcal{O}(g^8)$.

As a third example, consider dimension-eight terms. There now exist three possibilities. There are terms with six derivatives and two powers of the field, terms with four derivatives and four powers of the field, and terms with two derivatives and six powers of the field. The derivative interactions with two powers of the field and six powers of the field contribute at a higher order in the coupling whereas the interaction with four powers of the field contributes at $\mathcal{O}(g^4)$. It can be shown that the only independent derivative interaction with four derivatives and four powers of the field that contributes at $\mathcal{O}(g^4)$ is given by $(\partial\phi)^4$.

The only other possible terms that can contribute to $\mathcal{O}(g^4)$ are interactions constructed from four powers of the field with six or more derivatives and terms with six powers of the field and four or more derivatives. Terms with more than six powers of the field contribute to $\mathcal{O}(g^6)$ and higher and need not be considered.

Using the above illustrated techniques, one can proceed in a systematic fashion to determine the orders at which the various effective derivative interactions contribute. Therefore the effective Lagrangian, including both derivative and contact terms, can in principle, be calculated in a consistent fashion to any order in the coupling constant.

Chapter 5.
The Induced Thermal Mass at One-Loop Order

In this chapter, the induced thermal mass of a scalar field theory with a quartic coupling is computed to $\mathcal{O}(g^3)$. To illustrate the utility of the techinques developed in the previous chapters, the calculation is performed in the standard fashion and using the effective-Lagrangian approach. By doing so a comparison between the two methods can be made.

5.1. The Standard Method

The system that is studied in this chapter is described by the following Lagrangian density:

$$\mathcal{L} = -\frac{1}{2}\partial_\mu \phi(x)\,\partial^\mu \phi(x) - \frac{1}{4!}g^2\phi^4(x)\ . \tag{5.1.1}$$

The Lagrangian density given by Eq. (5.1.1) describes a massless scalar field with a quartic interaction. To compute the quantum and thermal corrections to the tree-level mass, one can employ the loop expansion. The one-loop correction to the mass is illustrated below in Fig. 5.1.1.

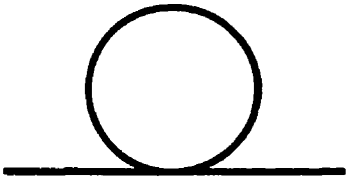

Figure 5.1.1: One-loop mass correction.

Using the finite-temperature Feynman rules, one finds that the correction to the two-point vertex function evaluated at zero four-momentum is given by:

$$\Gamma^2(0) = -\frac{g^2 T}{2(2\pi)^3}\sum_{n=-\infty}^{\infty}\int_0^\infty \frac{d^3\mathbf{k}}{k^2} \tag{5.1.2}$$

where $k^2 = k_0^2 + \mathbf{k}^2$ with $k_0 = 2\pi nT$. After performing the sum over n and the angular integral one obtains

$$\Gamma^2(0) = -\frac{g^2}{4\pi^2}\int_0^\infty \mathbf{k}^2 d|\mathbf{k}| \left(\frac{1}{2|\mathbf{k}|} + \frac{1}{|\mathbf{k}|\left(e^{|\mathbf{k}|/T}-1\right)}\right) . \tag{5.1.3}$$

The first term in Eq. (5.1.3) is a quadratically divergent quantity. Since this term does not depend on the temperature of the system, we can interpret it as the vacuum contribution to the mass of the scalar field. One can always choose the mass counterterm to precisely cancel this infinite quantity thus this term can be ignored. The second term is finite and is found to be

$$\Gamma^2(0) = -\frac{g^2}{4\pi^2}\int_0^\infty \frac{|\mathbf{k}|d|\mathbf{k}|}{\left(e^{|\mathbf{k}|/T}-1\right)} = -\frac{g^2T^2}{24} . \tag{5.1.4}$$

From Eq. (5.1.4) it follows that the scalar field develops a temperature-dependent mass, which to $\mathcal{O}(g^2)$ is given by

$$m_0^2(g,T) = \frac{g^2T^2}{24} . \tag{5.1.5}$$

If one now attempts to calculate the temperature-dependent mass correction to two-loop order or greater including loop momenta down to $\Lambda \leq \mathcal{O}(gT)$, severe infrared divergences will invalidate the loop expansion. For example, consider the following graphs which contribute to the two-point function at $\mathcal{O}(g^4)$.

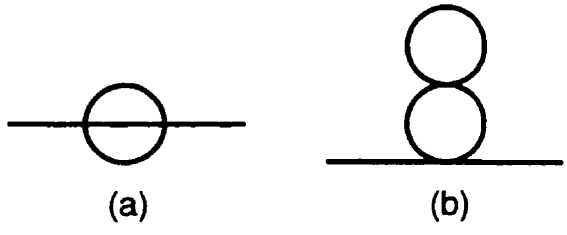

Figure 5.1.2: Two-loop mass corrections.

Graph (b) belongs to the set of "ring" graphs, and using the analysis from the previous chapter it is easy to verify that its contribution diverges as T/Λ, where

Λ is an infrared cutoff. It will be shown in the next chapter that the contribution from graph (a) diverges as $\log(T/\Lambda)$. Continuing in this manner one finds graphs which diverge as $(T/\Lambda)^3$ at three-loop order and $(T/\Lambda)^5$ at four-loop order. Thus at each order in the loop expansion there exist graphs that cannot be integrated over all momenta due to their infrared divergent behaviour. It turns out that all of the most divergent graphs belong to the set of "ring" graphs and it is possible to sum the entire series of ring graphs and to obtain a finite result[21].

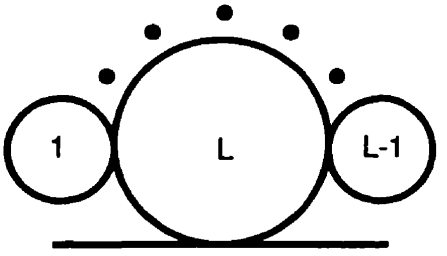

Figure 5.1.3: Ring-graph contribution to the two-point vertex.

A simple combinatoric analysis of Fig. 5.1.3, yields that the contribution of an L-loop ring graph is

$$\Gamma^{2,L}_{ring}(0) = \left(\frac{-g^2}{2}\right)^L T \sum_{n=-\infty}^{\infty} \int_0^{\infty} \frac{d^3\mathbf{k}}{(2\pi)^3} \frac{1}{k^2} \left(\frac{\Pi}{k^2}\right)^{L-1} \tag{5.1.6}$$

where Π is defined as

$$\Pi = T \sum_{n=-\infty}^{\infty} \int_0^{\infty} \frac{d^3\mathbf{k}}{(2\pi)^3} \frac{1}{k^2} = \frac{T^2}{12} \,. \tag{5.1.7}$$

Notice that each term with $L \geq 2$ is infrared divergent. Each contribution starting from $L = 1$ is a term in a geometric series, therefore the entire series can be summed to give the infrared-finite result

$$\Gamma^2_{ring}(0) = \frac{-g^2}{2} T \sum_{n=-\infty}^{\infty} \int_0^{\infty} \frac{d^3\mathbf{k}}{(2\pi)^3} \frac{1}{k^2 + m_0^2(g,T)} \tag{5.1.8}$$

with $m_0^2(g,T)$ defined in Eq. (5.1.5). The energy sum in Eq. (5.1.8) can be performed exactly, however, the momentum integration cannot be expressed in a simple closed-form. To simply examine its features a high-temperature expansion is employed[45]. One can expand Eq. (5.1.8) in powers of $m_0(g,T)/T$ as

$$\Gamma^2_{ring}(0) = -\frac{g^2T^2}{24}\left(1 - \frac{3m_0(g,T)}{\pi T} + \mathcal{O}\left(\frac{m_0^2(g,T)}{T^2}\right)\right) \tag{5.1.9}$$

to find that the induced thermal mass to $\mathcal{O}(g^3)$ is given by

$$m^2(g,T) = \frac{g^2T^2}{24}\left(1 - \frac{3m_0(g,T)}{\pi T}\right) + \mathcal{O}(g^4) \tag{5.1.10}$$

which agrees with the result obtained by Dolan and Jackiw[46].

It is an interesting fact that the next-to-leading order correction is of $\mathcal{O}(g^3)$ and not of $\mathcal{O}(g^4)$. The expectation of a series in g^2 is incorrect. The infinite sum of infrared divergent graphs has yielded an answer that is nonanalytic in the coupling g^2. An interesting question that needs to be addressed is: Can a reorganization of the perturbative expansion eliminate the need for summing an infinite number of diagrams? In other words, if we were all "combinatoric cripples"[47] could we compute the $\mathcal{O}(g^3)$ correction? This is an important question because in order to sum an infinite number of graphs one must also argue that there are no other graphs as important as those being summed. The answer to this question is yes. The renormalization group can perform the needed summation.

In the next section, we will illustrate how the application of the renormalization-group equation will sum the infinite set of "ring" diagrams. To achieve this, one must first derive the effective Lagrangian to $\mathcal{O}(g^2)$ by "integrating out" the modes with $p^2 \geq \Lambda^2$ where $T > \Lambda \gg \mathcal{O}(gT)$ is the infrared cutoff for the original theory described by Eq. (5.1.1). The next-to-leading order correction to the induced thermal mass is obtained by computing the one-loop correction using the effective theory. The form of the result can be obtained, up to integration constants, by applying the renormalization-group equation. If the calculation is carried out explicitly, then the result given by Eq. (5.1.10) is obtained.

5.2. The Effective-Lagrangian Approach

The first step in deriving the effective-Lagrangian for the theory described by Eq. (5.1.1) is to decide to which order the effective theory must be valid. We choose the cutoff such that $gT \ll \Lambda < T$. This ensures that one maintains perturbative calculability in the high-energy theory. As a first approximation, we will derive the effective theory to $\mathcal{O}(g^2)$. The next order of approximation is $\mathcal{O}(g^4)$ because one does have a series in g^2 in the high-energy theory. This accuracy is not needed to obtain the next-to-leading order correction to the induced thermal mass. As explained in chapter four, to obtain the effective Lagrangian to $\mathcal{O}(g^2)$, only the one-loop correction to the two-point function and the tree-level contribution to the four-point function are required.

At this point, we would like to integrate over all modes with Euclidean-signature four-momentum p satisfying $p^2 > \Lambda^2$ in the one-loop two-point vertex. To do this, we must sum over all $n \neq 0$ in the energy sum and only integrate over $\mathbf{p}^2 > \Lambda^2$ in the $n = 0$ mode. Recall that $\Lambda < T$, therefore all modes with $n \neq 0$ satisfy $p^2 > \Lambda^2$ whereas only the modes with $\mathbf{p}^2 > \Lambda^2$ satisfy $p^2 > \Lambda^2$ in the $n = 0$ contribution. Since the complete sum and momentum integration has been performed in deriving Eq. (5.1.4), all that is required is that we subtract the contribution from modes with $\mathbf{p}^2 < \Lambda^2$ from the result. Therefore the tree-level contrbution to the two-point vertex in the effective theory is given by

$$\Gamma^2_\Lambda(0) = -\frac{g^2T^2}{24} + \frac{g^2T}{4\pi^2}\int_0^\Lambda d|\mathbf{k}| \,. \tag{5.2.1}$$

The effective mass to $\mathcal{O}(g^2)$ is simply

$$m^2_\Lambda = \frac{g^2T^2}{24} - \frac{g^2T\Lambda}{4\pi^2} \,. \tag{5.2.2}$$

We can now express the effective-Lagrangian density accurate to $\mathcal{O}(g^2)$ as

$$\mathcal{L}(\Lambda, T) = -\frac{1}{2}\partial_\mu\phi(x)\,\partial^\mu\phi(x) - \frac{1}{2}m^2_\Lambda\phi^2(x) - \frac{1}{4!}g^2\phi^4(x) + \mathcal{O}\left(g^4\right) \,. \tag{5.2.3}$$

At this point, we choose to keep the cutoff-dependent mass term found in Eq. (5.2.2) in the unperturbed sector of the theory and treat all other terms as

perturbations. The reason for keeping the mass term in the unperturbed sector is to prevent the occurence of the infrared divergences which ruin perturbation theory. It should be stressed that Eq. (5.1.1) and Eq. (5.2.3) describe exactly the same physics. The reorganization of the perturbation theory has now been achieved since the effective degrees of freedom of the new equivalent theory are very different from the original massless theory. The Feynman rules of the effective theory differ from the original rules in the following ways. The propagator of the effective theory is that of a massive scalar field unlike that of the original Lagrangian density. Instead of having only a four point interaction, we now have an infinite number of interactions with cutoff-dependent and temperature-dependent coupling constants whose strengths can be determined in a consistent fashion. Since we are only working to $\mathcal{O}(g^2)$, these other effective interactions are not needed in what follows. In the effective theory, to calculate a particular Green's function to any given order in the coupling constant, only a finite number of interactions need to be considered. Since the effective theory is the low-energy theory, the propagator can only carry four-momentum p such that $p^2 < \Lambda^2$.

To calculate the next-to-leading order correction to the effective mass using the effective theory one can employ the loop expansion. The loop expansion in the high-energy theory has the property that one gains an extra factor of g^2 for each extra loop in a diagram. This is not the case with the low-energy effective theory. In the effective theory, one only gains an extra factor of g for every extra loop. To see that this is in fact the case, consider the expression for the L-loop ring graph contribution to the two-point vertex in the low-energy theory. These graphs are sufficient to make our point since, as already shown, they are the most infrared divergent. Using Eq. (5.1.6) as a guide, we obtain

$$\Gamma^{2,L}_{ring}(0,\Lambda,T) = \left(\frac{-g^2}{2}\right)^L T \int_0^\Lambda \frac{d^3\mathbf{k}}{(2\pi)^3} \frac{1}{(\mathbf{k}^2+m_\Lambda^2)} \left(\frac{\Pi_\Lambda}{(\mathbf{k}^2+m_\Lambda^2)}\right)^{L-1} \tag{5.2.4}$$

where Π_Λ is defined as

$$\Pi_\Lambda = T \int_0^\Lambda \frac{d^3\mathbf{k}}{(2\pi)^3} \frac{1}{(\mathbf{k}^2+m_\Lambda^2)} \sim \Lambda T + \mathcal{O}(g) \ . \tag{5.2.5}$$

At this point it is useful to introduce the following dimensionless variables:

$$\mu = \frac{m_\Lambda}{T} \qquad \lambda = \frac{\Lambda}{T} \qquad z = \frac{\lambda}{\mu} \,. \tag{5.2.6}$$

The only constraint on Λ is that it be chosen to satisfy $T > \Lambda \gg gT$ where the coupling constant g is a very small number. From this it follows that $1/\mu > z \gg 1$. Actually, one can always choose λ such that $1/\mu > z^n \gg 1$ for any value of n. This is achieved by choosing λ such that $\mu^{\frac{n-1}{n}} > \lambda \gg \mu$. From this fact it follows that one can always express the contributions of the low-energy theory as a power of the coupling g multiplied by a polynomial function in z and $\log(z)$.

Substituting the variables given by Eq. (5.2.6) in Eq. (5.2.4), one finds that

$$\frac{\Gamma^{2,L}_{ring}(0,\Lambda,T)}{T^2} \sim \mu^2 \left(\frac{g^2}{\mu}\right)^L S(z) \tag{5.2.7}$$

where $S(z)$ is a function of z that has the following schematic form

$$S(z) \sim z^{L-1} \int_0^z \frac{x^2 dx}{(x^2+1)^L} \,. \tag{5.2.8}$$

It is easy to see that the function $S(z)$ can always be expressed as a polynomial in z and $\log(z)$. Using the fact that $\mu \sim g$, it is easy to see that Eq. (5.2.7) gains a factor of g for every extra loop. When $L = 0$ the contribution is of $\mathcal{O}(g^2)$, as expected. For $L = 1$, one finds that the correction is of $\mathcal{O}(g^3)$, which is the correction we want to compute. Continuing in this manner, one can compute quantities to any order in g by considering only a finite number of diagrams. Therefore one does have a well defined perturbation theory in the low-energy regime if one considers the contributions to be given by powers of g multiplied by a function of z.

One can also use Eq. (5.2.8) to obtain the leading large z behaviour for the function $S(z)$. For example, for $L = 1$ Eq. (5.2.8) implies that the leading behaviour is linear in z. For $L = 2$ the leading behaviour is also linear in z. At $L = 3$ the dominant behaviour is quadratic in z and one gains an extra power of z for every extra loop after $L = 3$.

5.2.1. Using the Renormalization-Group Equation

We are now in a position to compute the correction to the two-point vertex using the effective theory. The two-point vertex can be written in the following manner;

$$\frac{\Gamma^2(0)}{T^2} = -\mu^2 + \mu g^2 S_1(z) + \mathcal{O}\left(g^4, z\right) \tag{5.2.9}$$

where $S_1(z)$ is a function of z that will be determined by the application of the renormalization-group equation. The first term in Eq. (5.2.9) represents the tree-level contribution to the two-point vertex in the effective theory. The second term represents the one-loop correction to the two-point vertex computed within the effective theory and the third term represents corrections from diagrams with two or more loops. We also know that the two-loop correction is at most linear in z. The sum of the first two terms gives the two-point vertex accurate to $\mathcal{O}(g^3)$, which must be independent of λ. The structure of the one-loop correction is easily understood. There is a factor of g^2 because the one-loop correction involves only one vertex. The factor of μ is due to the fact that the loop integral is three dimensional and there is only one propagator. After one factors out the effective mass from the loop integral and divides by T^2, a factor of μ will remain multiplied by a dimensionless integral whose upper limit of integration is $z = \lambda/\mu$.

By applying Eq. (3.3.3), the renormalization-group equation, to Eq. (5.2.9), one can obtain the large-z form of the function $S_1(z)$ without the explicit evaluation of Feynman graphs. Applying the renormalization-group equation to Eq. (5.2.9) yields

$$\frac{g^2}{4\pi^2} - \frac{g^4}{8\pi^2\mu} S_1(z) + g^2 \frac{d}{dz} S_1(z) + \frac{g^4 z}{8\pi^2\mu} \frac{d}{dz} S_1(z) + \mathcal{O}\left(g^3\right) = 0\,. \tag{5.2.10}$$

In obtaining Eq. (5.2.10), we have used the following relationships:

$$\frac{d\mu}{d\lambda} = \frac{-g^2}{8\pi^2\mu} + \mathcal{O}\left(g^3/\lambda^2\right) \qquad \frac{dz}{d\lambda} = \frac{1}{\mu}\left(1 + \frac{g^2 z}{8\pi^2\mu} + \mathcal{O}\left(g^2/\lambda\right)\right) \tag{5.2.11}$$

where the derivatives are taken with g fixed. The correction of $\mathcal{O}(g^3)$ appearing in Eq. (5.2.10) is due to the derivative of the two-loop correction taken with respect to λ. The solution of Eq. (5.2.10) for $S_1(z)$ is easily obtained by inspection, and found to be

$$S_1(z) = -\frac{z}{4\pi^2} + C + \mathcal{O}(1/z) \tag{5.2.12}$$

for large z.

As expected from our general arguments, the leading behaviour of $S_1(z)$ is linear in z. The integration constant C can be determined in at least two ways. One can evaluate the one-loop graph explicitly, as will be done in the next subsection, or using knowledge of the two-loop correction. If one had the leading behaviour for the two-loop correction, one would find that the constant C must have a value such that the $\mathcal{O}(g^3)$ correction in Eq. (5.2.10) vanishes. When we extend our analysis to two-loop order, we will find that this is true. We will now determine the function $S_1(z)$ by evaluating the one-loop Feynman graph.

5.2.2. The Explicit Calculation

Using the Feynman rules of the effective theory, one finds that the one-loop correction to the tree-level two-point function is

$$\Gamma^2(0,\Lambda,T) = \frac{-g^2T}{2}\int_0^\Lambda \frac{d^3\mathbf{k}}{(2\pi)^3}\frac{1}{\left(\mathbf{k}^2+m_\Lambda^2\right)}\,. \tag{5.2.13}$$

Using the variables defined by Eq. (5.2.6), one can rewrite Eq. (5.2.13) as

$$\frac{\Gamma^2(0,z)}{T^2} = \frac{-g^2\mu}{4\pi^2}\int_0^z \frac{x^2dx}{(x^2+1)}\,. \tag{5.2.14}$$

The integral can be performed easily to yield

$$\frac{\Gamma^2(0,z)}{T^2} = \frac{-g^2\mu}{4\pi^2}\left(z-\arctan(z)\right)\,. \tag{5.2.15}$$

By comparing to Eq. (5.2.9), we find that the exact solution for $S_1(z)$ is given by

$$S_1(z) = -\frac{z}{4\pi^2}+\frac{1}{4\pi^2}\arctan(z) \tag{5.2.16}$$

which can be expanded for large z as

$$S_1(z) = -\frac{z}{4\pi^2}+\frac{1}{8\pi}-\frac{1}{4\pi^2 z}+\frac{1}{12\pi^2 z^3}+\cdots\,. \tag{5.2.17}$$

Thus our expression for $S_1(z)$ obtained by using the renormalization group agrees with the explicit one-loop result. The value of the integration constant C is found to be $C = 1/8\pi$. The induced thermal mass calculated to one-loop order in the

effective theory can be obtained by substituting Eq. (5.2.17) into Eq. (5.2.9) which results in

$$\frac{\Gamma^2(0)}{T^2} = -\mu^2 + \mu g^2 \left(-\frac{z}{4\pi^2} + \frac{1}{8\pi} + \mathcal{O}(1/z) \right) . \tag{5.2.18}$$

The expression for μ^2 is obtained by dividing Eq. (5.2.2) by T^2 and the result can be substituted in Eq. (5.2.18) to give

$$\frac{\Gamma^2(0)}{T^2} = -\frac{g^2}{24} + \frac{g^2\lambda}{4\pi^2} - \frac{g^2\mu z}{4\pi^2} + \frac{g^2\mu}{8\pi} + \mathcal{O}(g^4) . \tag{5.2.19}$$

By using the fact that $z = \lambda/\mu$ we find that the explicit λ dependence cancels at $\mathcal{O}(g^2)$ and that the two-point vertex at one-loop order is

$$\frac{\Gamma^2(0)}{T^2} = -\frac{g^2}{24} + \frac{g^2\mu}{8\pi} + \mathcal{O}(g^4) . \tag{5.2.20}$$

One can also make use of the fact that μ can be expanded as

$$\mu = \frac{g}{\sqrt{24}} (1 + \mathcal{O}(g)) . \tag{5.2.21}$$

Substituting Eq. (5.2.21) into Eq. (5.2.20) and neglecting terms of $\mathcal{O}(g^4)$, the induced thermal mass at one-loop order is found to be

$$m^2(g,T) = \frac{g^2T^2}{24} \left(1 - \frac{3m_0(g,T)}{\pi T} \right) + \mathcal{O}(g^4) \tag{5.2.22}$$

where m_0^2 is defined by Eq. (5.1.5). The result obtained using the effective theory is identical to that given by Eq. (5.1.10).

Recall that an infinite number of infrared-divergent graphs needed to be summed in order to obtain the mass at $\mathcal{O}(g^3)$ using the original theory. Within the effective theory, only one infrared-finite graph needs to be evaluated. Thus an infinite number of graphs have been resummed in the effective theory. The fact that an infinite number of graphs have been resummed within the effective theory can be seen by studying Eq. (5.2.15). By expanding the arctangent function for large z, it is easy to show that

$$\frac{\Gamma^2(0,z)}{T^2} = \frac{-g^2\mu z}{4\pi^2} + \frac{g^2\mu}{8\pi} + \frac{g^2\mu}{4\pi^2} \sum_{n=1}^{\infty} \frac{(-1)^n}{(2n-1)\, z^{2n-1}} . \tag{5.2.23}$$

If one then considers Eq. (5.1.6) which is the expression for the L-loop ring graph contributions from the high-energy theory, one can show that infrared divergent terms are given by the equation

$$\Gamma^{2,n}_{HE}(0,\Lambda) = \frac{-g^2}{2}\left(\frac{-g^2}{2}\right)^n \left(\frac{T^2}{12} - \frac{T\Lambda}{2\pi^2}\right)^n \left(\frac{T}{2\pi^2}\right) \int_{\Lambda}^{\infty} \frac{d|\mathbf{k}|}{\mathbf{k}^{2n}} \tag{5.2.24}$$

where $n = L - 1$. Using the definition of m_Λ^2 and performing the integration gives

$$\Gamma^{2,n}_{HE}(0,\Lambda) = -\frac{g^2 T m_\Lambda}{4\pi^2}(m_\Lambda)^{2n-1}(-1)^n \left(\frac{1}{(2n-1)\,\Lambda^{2n-1}}\right) . \tag{5.2.25}$$

The sum of all the infrared-divergent ring graphs is

$$\Gamma^{2}_{HE}(0,z) = -\frac{g^2 T m_\Lambda}{4\pi^2}\sum_{n=1}^{\infty} \frac{(-1)^n}{(2n-1)\,z^{2n-1}} \tag{5.2.26}$$

where the change of variable $z = \Lambda/m_\Lambda$ has been made. To show that the infrared-divergent terms from the high-energy theory are cancelled by terms in the low-energy theory, divide Eq. (5.2.26) by T^2 to obtain

$$\frac{\Gamma^{2}_{HE}(0,z)}{T^2} = -\frac{g^2 \mu}{4\pi^2}\sum_{n=1}^{\infty} \frac{(-1)^n}{(2n-1)\,z^{2n-1}} \tag{5.2.27}$$

which precisely cancels the terms in Eq. (5.2.23). Thus all the contributions of the infrared-divergent ring graphs are included in the one-loop correction of the effective theory. The perturbation theory has been reorganized by integrating out the high-frequency modes and keeping the effective mass in the unperturbed sector of the Lagrangian. This reorganization allows one to compute the mass corrections perturbatively, in powers of g, without considering an infinite number of graphs. This is an important point because this gives one much better control over which Feynman graphs have been neglected. The dominant behaviour of the low-energy contributions can be obtained by using simple power-counting arguments and employing the renormalization-group equation. We will now extend our analysis by evaluating the induced thermal mass at two-loop order in the effective theory.

Chapter 6.
The Induced Thermal Mass at Two-Loop Order

In this chapter, the $\mathcal{O}(g^4)$ contributions to the induced thermal mass that have a singular dependence on g are determined by using a renormalization-group approach. This technique is employed because it allows one to determine the dominant contributions with reasonable ease. Although the integration constants cannot be determined without an explicit calculation, the dominant logarithmic term can be isolated without much effort.

6.1. Deriving The Effective Theory

As in chapter five, the system that is studied is described by the following Lagrangian density:

$$\mathcal{L} = -\frac{1}{2}\partial_\mu\phi(x)\,\partial^\mu\phi(x) - \frac{1}{4!}g^2\phi^4(x)\ . \tag{6.1.1}$$

The goal is to compute the induced thermal mass to $\mathcal{O}(g^4)$. Since Eq. (6.1.1) describes a theory of massless interacting particles, we know that terms within the standard perturbative expansion are infrared divergent. Thus to reorganize the theory, we will derive an effective Lagrangian density. The Lagrangian density that is needed must be consistent to $\mathcal{O}(g^4)$ because that is the order to which the mass must be evaluated.

Using the arguments presented in chapter four, we know that to obtain the effective theory accurate to $\mathcal{O}(g^4)$ that the following changes must be made. One must integrate over all high-frequency modes in the two-point function at both one and two-loop order. The high-energy modes must be integrated out at one-loop order in the four-point function. We must also include derivative interactions constructed from four powers of the field ϕ and four or more derivatives. Finally, a new effective six-point contact interaction is needed in the effective theory along with six-point derivative interactions with four or more derivatives. We will now present each of the above mentioned changes and discuss their contributions to the terms with singular g dependence.

6.1.1. Corrections to the Two-Point Function

The high-frequency modes need to be integrated out in the following diagrams:

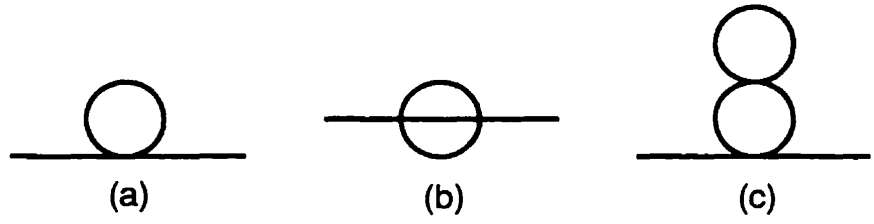

Figure 6.1.1: Corrections to the two-point function.

If we choose to integrate out the modes with $p^2 > \Lambda^2$ with $gT \ll \Lambda < T$ then the result for diagram (a) is given by Eq. (5.2.1). When one integrates over the high-energy modes in diagram (b) and removes the UV-divergent contributions with the mass and wave-function renormalization counterterms, one finds that the contribution can be written as

$$\Gamma_{\Lambda}^{2,2b}(0) = g^4T^2F_1 + g^4T^2F_2(T,\Lambda) + g^4T^2F_3(T,\Lambda) \ . \tag{6.1.2}$$

In the above equation F_1 is a constant, $F_2(T,\Lambda)$ is a function that vanishes in the limit $\Lambda \to 0$ and contains only positive powers of Λ, and the function $F_3(T,\Lambda)$ diverges in the limit $\Lambda \to 0$ and contains only negative powers of Λ and any non-analytic Λ dependence. The reason for expressing the two-point function in this manner is as follows. Since the cutoff Λ is chosen to be less than the temperature T of the system, all contributions in the energy sums with $n \neq 0$ have no Λ dependence due to they way the cutoff has been defined. These contributions are therefore constants. Only the $n = 0$ contributions with $\mathrm{p}^2 > \Lambda^2$ are sensitive to the infrared cutoff Λ. Thus these contributions can include constants, terms which are finite as $\Lambda \to 0$ and terms which diverge as $\Lambda \to 0$. The value of the constant F_1 and the functional forms of $F_2(T,\Lambda)$ and $F_3(T,\Lambda)$ are not needed, the important point is to have separated the three contributions by their behaviour as $\Lambda \to 0$. There are also momentum-dependent terms from diagram (b), however, these can be interpreted as derivative interactions and do not contribute to $\mathcal{O}(g^4)$.

Similarly, the contribution from diagram (c) may also be written as

$$\Gamma_{\Lambda}^{2,2c}(0) = g^4T^2G_1 + g^4T^2G_2(T,\Lambda) + g^4T^2G_3(T,\Lambda) \tag{6.1.3}$$

where G_1, G_2, and G_3 have been defined in a manner similar to F_1, $F_2(T,\Lambda)$, and $F_3(T,\Lambda)$. Summing the contributions from the three diagrams and multiplying by -1 yields an effective mass accurate to $\mathcal{O}(g^4)$ of

$$m_{\Lambda}^2 = \frac{g^2T^2}{24} - \frac{g^2T\Lambda}{4\pi^2} + g^4T^2H_1 + g^4T^2H_2(T,\Lambda) + g^4T^2H_3(T,\Lambda) \tag{6.1.4}$$

where, as before, H_1, $H_2(T,\Lambda)$, and $H_3(T,\Lambda)$ are defined in a manner similar to G_1, G_2, and G_3. Since we are interested in calculating the terms with singular g dependence, we can ignore the terms proportional to H_1 and $H_2(T,\Lambda)$.

6.1.2. Corrections to the Four-Point Function

We must now integrate over the high-energy modes in the following one-loop diagrams.

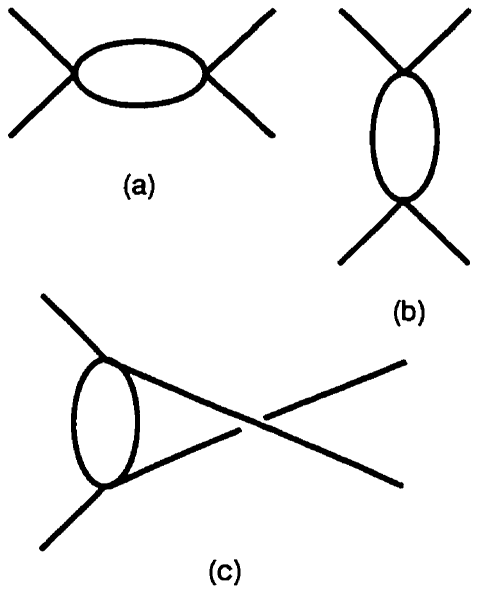

Figure 6.1.2: 1-loop corrections to the four-point function.

Using the same reasoning as with the corrections to the two-point function, we can express the $\mathcal{O}(g^4)$ correction to the coupling constant as

$$\Gamma_{\Lambda}^{4}(0) = g^4I_1 + g^4I_2(T,\Lambda) + g^4I_3(T,\Lambda) \tag{6.1.5}$$

where, as before, I_1, $I_2(T,\Lambda)$, and $I_3(T,\Lambda)$ are defined by their behaviour similar to G_1, G_2, and G_3. It should be stressed that the UV-divergent contributions to the four-point function are removed by the coupling-constant counterterm. The four-point coupling constant in the effective theory, accurate to $\mathcal{O}(g^4)$, is given by

$$g_\Lambda^2 = g^2 + g^4 J_1 + g^4 J_2\,(T,\Lambda) + g^4 J_3\,(T,\Lambda) \tag{6.1.6}$$

with J_1, $J_2(T,\Lambda)$, $J_3(T,\Lambda)$ exhibiting the same behaviour as I_1, $I_2(T,\Lambda)$ and $I_3(T,\Lambda)$ respectively.

There are also derivative interactions involving four powers of the field and four or more derivatives. These interactions contribute to the induced thermal mass through a one-loop mass correction. The derivative interactions will appear as momentum-dependent vertices, therefore, the one-loop mass correction will be proportional to some power of the external momentum. To determine the induced thermal mass, we can take the external momentum to be zero, and therefore, the contributions to the mass will vanish. For this reason, all derivative interactions involving four powers of the field and four or more derivatives can be ignored.

6.1.3. The Effective Six-Point Interaction

The final contributions to the effective theory are effective six-point interactions. As already explained, these interactions is needed to compensate for the removal of high-frequency modes in scattering processes such as the one depicted below.

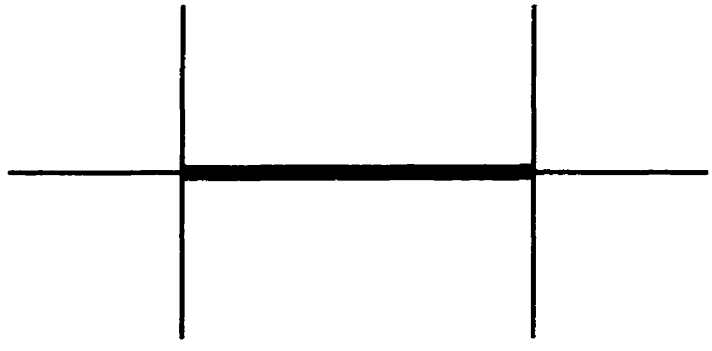

Figure 6.1.3: Six-particle scattering in ϕ^4 theory.

To show that the effective six-point contact interaction is needed, we will compute the six-particle scattering amplitude given by Fig. 6.1.3 in both the high-energy and low-energy theories. We will find that the amplitudes differ at high-momentum transfer thus indicating the need for the effective six-point interaction. The amplitude for this process computed in the original massless theory goes like

$$A_{HE}\left(p^2\right) \sim \frac{g^4}{p^2} \tag{6.1.7}$$

where the four-momentum p is the exchange momentum carried by the internal line. In the original theory, the exchange momentum p can take any value. In the effective theory, however, the exchange momentum is cut off at a scale Λ by the cutoff function $K(p^2/\Lambda^2)$. Thus the contribution from Fig. 6.1.3 in the low-energy effective theory is

$$A_{LE}\left(p^2\right) \sim \frac{g^4}{p^2+m_\Lambda^2} K\left(p^2/\Lambda^2\right) \ . \tag{6.1.8}$$

When the exchange momentum p is such that $\Lambda^2 > p^2 > m_\Lambda^2$ then Eq. (6.1.7) and Eq. (6.1.8) agree at $\mathcal{O}(g^4)$ with an error of $\mathcal{O}(g^4 m_\Lambda^2/p^2)$. When the exhange momentum p is such that $p^2 > \Lambda^2$ then the two amplitudes will differ at $\mathcal{O}(g^4)$. This difference occurs because the high-frequency modes do not propagate along the internal line in the effective theory. Although each of the external momenta are less than the cutoff, their sum can be greater than the cutoff. To compensate for this difference, one must add an effective six-point interaction to the low-energy theory. The contribution to six-particle scattering in the effective theory is now given by

$$A_{LE}\left(p^2\right) \sim \frac{g^4}{p^2+m_\Lambda^2} K\left(p^2/\Lambda^2\right) + C_6\left(g,\Lambda,p\right) \tag{6.1.9}$$

where $C_6(g,\Lambda,p)$ is the coefficient of the $\phi^6(x)$ term in the effective theory. If the coefficient function $C_6(g,\Lambda,p)$ is chosen correctly, then the amplitudes given by Eq. (6.1.7) and Eq. (6.1.9) will agree at $\mathcal{O}(g^4)$. One can solve for the coefficient function by choosing a specific form for the cutoff function $K(p^2/\Lambda^2)$, equating Eq. (6.1.7) and Eq. (6.1.9) and then solving for $C_6(g,\Lambda,p)$. Solving for $C_6(g,\Lambda,p)$ yields

$$C_6\left(g,\Lambda,p\right) \sim \frac{g^4}{\Lambda^2}\left(1+\mathcal{O}\left(\frac{p^2}{\Lambda^2}\right)\right) \ . \tag{6.1.10}$$

The terms with momentum dependence in Eq. (6.1.10) can be interpreted as derivative interactions and they will be considered next. Therefore, to leading order, an effective six-point interaction given by

$$-\frac{g^4}{6!}\left(\frac{c}{\Lambda^2}\right)\phi^6(x)$$

where c is a constant, must be included in the effective theory.

We must now consider the importance of derivative interactions constructed from six powers of the field and four or more derivatives. These interactions can contribute to the induced thermal mass through two-loop diagrams. The derivative interaction with four derivatives can, at most, contribute a constant at $\mathcal{O}(g^4)$. Since this is nonsingular in the coupling g, it can be ignored. The two-loop diagrams constructed from vertices with six or more derivatives will be proportional to the external momentum. As before, we can take the external momentum to be zero and therefore also ignore these contributions.

Combining all of the above mentioned changes, one finds that the Lagrangian density for the low-energy effective theory is given by

$$\mathcal{L}(\Lambda,T)=-\frac{1}{2}\partial_\mu\phi(x)\,\partial^\mu\phi(x)-\frac{1}{2}m_\Lambda^2\phi^2(x)-\frac{1}{4!}g_\Lambda^2\phi^4(x)-\frac{g^4}{6!}\left(\frac{c}{\Lambda^2}\right)\phi^6(x)+\mathcal{O}\left(g^6\right) \tag{6.1.11}$$

with m_Λ^2 and g_Λ^2 defined by Eq. (6.1.4) and Eq. (6.1.6) respectively. It must be stressed that this is not the complete Lagrangian density at $\mathcal{O}(g^4)$ since we have neglected to include the derivative interactions. This Lagrangian is complete for the purposes of computing the $\mathcal{O}(g^4)$ terms in the induced thermal mass that have a singular dependence on the coupling g.

6.2. Calculating The Induced Thermal Mass

To compute the induced thermal mass with the effective theory, one can use the loop expansion. The contributions to the two-point function, evaluated at zero external momentum, are given by

$$\frac{\Gamma^2(0)}{T^2}=-\mu^2+\mu g_\Lambda^2 S_1(z)+g_\Lambda^4 S_2(z)+\mathcal{O}\left(g^6/\mu,z^2\right) \tag{6.2.1}$$

where the variables μ, λ and z are defined by

$$\mu = \frac{m_\Lambda}{T} \qquad \lambda = \frac{\Lambda}{T} \qquad z = \frac{\lambda}{\mu}\,. \tag{6.2.2}$$

The first term in Eq. (6.2.1) is due to the tree-level mass in the effective theory. The second term is the one-loop correction constructed from the four-point interaction. The third term represents two-loop corrections constructed from two four-point vertices. There is also a two-loop diagram constructed from one six-point vertex, however, this contributes a constant at $\mathcal{O}(g^4)$ and can be ignored. These corrections are represented by the Feynman graphs presented below. The final term represents the dominant corrections from diagrams with three or more loops. These errors are of $\mathcal{O}(g^5)$ because $\mu \sim \mathcal{O}(g)$.

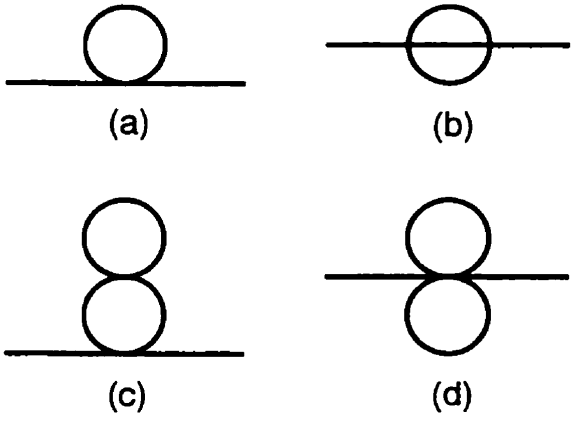

Figure 6.2.1: One-loop and two-loop corrections to the two-point function in the effective theory.

Our aim is to solve for $S_2(z)$ without evaluating the Feynman diagrams explicitly. To achieve this, we can apply the renormalization-group equation to Eq. (6.2.1) and solve for $S_2(z)$. Before taking the derivative with respect to λ one must substitute the expressions for μ^2, g_Λ^2 and $S_1(z)$ into Eq. (6.2.1). It is important to expand $S_1(z)$ to at least $\mathcal{O}(1/z)$ to be consistent at $\mathcal{O}(g^4)$. After making the above mentioned

substitutions, one obtains

$$\begin{aligned}\frac{\Gamma^2(0)}{T^2} = &-\frac{g^2}{24}+\frac{g^2\lambda}{4\pi^2}+g^4G_3 \\ &+\mu g^2\left(1+g^2\left(J_1+J_2+J_3\right)\right)\left(-\frac{z}{4\pi^2}+\frac{1}{8\pi}-\frac{1}{4\pi^2 z}+\mathcal{O}\left(1/z^3\right)\right) \\ &+g^4\left(1+g^2\left(J_1+J_2+J_3\right)\right)^2 S_2(z)+\mathcal{O}\left(g^6/\mu,z^2\right)\end{aligned} \tag{6.2.3}$$

where the functions G_3, J_1, J_2 and J_3 are defined in Eq. (6.1.3) and Eq. (6.1.4). If one discards all terms of $\mathcal{O}(g^5)$ and higher, then Eq. (6.2.3) simplifies to

$$\begin{aligned}\frac{\Gamma^2(0)}{T^2} = &-\frac{g^2}{24}+\frac{g^2\lambda}{4\pi^2}+g^4G_3+\mu g^2\left(-\frac{z}{4\pi^2}+\frac{1}{8\pi}-\frac{1}{4\pi^2 z}+\mathcal{O}\left(1/z^3\right)\right) \\ &+g^4S_2(z)+\mathcal{O}\left(g^6/\mu,z^2\right)\ .\end{aligned} \tag{6.2.4}$$

By using the fact that $z=\lambda/\mu$, Eq. (6.2.4) can be rewritten as

$$\frac{\Gamma^2(0)}{T^2} = -\frac{g^2}{24}+g^4G_3-\frac{\mu^2g^2}{4\pi^2\lambda}+\frac{\mu g^2}{8\pi}+g^4S_2(z)+\mathcal{O}\left(g^6/\mu,z^2\right) \tag{6.2.5}$$

where terms that have been discarded are $\mathcal{O}(g^6)$ and greater. Further progress can be made by substituting the lowest order expression for μ^2 into Eq. (6.2.5) to obtain

$$\frac{\Gamma^2(0)}{T^2} = -\frac{g^2}{24}+g^4G_3-\frac{g^4}{96\pi^2\lambda}+\frac{g^4}{16\pi^4}+\frac{\mu g^2}{8\pi}+g^4S_2(z)+\mathcal{O}\left(g^6/\mu,z^2\right)\ . \tag{6.2.6}$$

The renormalization-group equation, given by Eq. (3.3.3), can now be applied to Eq. (6.2.6), which demands the $\Gamma^2(0)$ be independent of λ. Taking a derivative with respect to λ, we obtain

$$g^4\frac{d}{d\lambda}\left(G_3(\lambda)-\frac{1}{96\pi^2\lambda}\right)+\frac{g^2}{8\pi}\left(\frac{d\mu}{d\lambda}\right)+g^4\left(\frac{dz}{d\lambda}\right)\frac{d}{dz}S_2(z)+\mathcal{O}\left(g^4,z\right)=0 \tag{6.2.7}$$

where we have used the fact that $dz/d\lambda \sim 1/g$ in the estimate of the error. One can now substitute the expressions for $d\mu/d\lambda$ and $dz/d\lambda$ given by Eq. (5.2.11) into Eq. (6.2.7) to yield

$$g^4\frac{d}{d\lambda}\left(G_3(\lambda)-\frac{1}{96\pi^2\lambda}\right)-\frac{g^4}{64\pi^3\mu}+\frac{g^4}{\mu}\frac{d}{dz}S_2(z)+\frac{g^6\lambda}{8\pi^2\mu^3}\frac{d}{dz}S_2(z)+\mathcal{O}\left(g^4,z\right)=0\ . \tag{6.2.8}$$

It is easy to verify that the solution for $S_2(z)$, for large z, is given by

$$S_2(z)=\frac{z}{64\pi^3}+C_1\log(z)+C_2+\mathcal{O}(1/z) \tag{6.2.9}$$

where

$$C_1 = -\lambda \frac{d}{d\lambda}\left(G_3(\lambda) - \frac{1}{96\pi^2\lambda}\right) \tag{6.2.10}$$

and C_2 is an integration constant. Notice that the constant of $\mathcal{O}(g^3)$, the second term in Eq. (6.2.8), is cancelled by the third term. This is the cancellation that could have been used to determine the integration constant in the one-loop calculation if one had knowledge of the leading behaviour of the two-loop corrections.

To solve for the induced thermal mass at $\mathcal{O}(g^4)$, all that is required is that the expression for $S_2(z)$ be substituted into Eq. (6.2.1). Before doing so, however, we would like to solve for the constant C_1 which is the coefficient of the logarithmic term in $S_2(z)$. To determine the constant C_1, one can use Eq. (6.2.10) which requires the explicit form of the function $G_3(\lambda)$. Recall that the function $G_3(\lambda)$ represents the $\mathcal{O}(g^4)$ terms that diverge in the limit $\lambda \to 0$ in the two-point function. The function $G_3(\lambda)$ is determined in the next subsection.

6.2.1. Extracting The Coefficient of The Logarithmic Term

To determine the function $G_3(\lambda)$, one must integrate over the high-frequency modes in diagrams (b) and (c) of Fig. 6.1.1. Using the Feynman rules previously presented, the contribution of diagram (c) is

$$\Gamma^{2,c}(0) = \frac{g^4}{4}\left(T\sum_{n=-\infty}^{\infty}\int_{\Lambda}^{\infty}\frac{d^3\mathbf{k}}{(2\pi)^3 k^4}\right)\left(T\sum_{m=-\infty}^{\infty}\int_{\Lambda}^{\infty}\frac{d^3\mathbf{p}}{(2\pi)^3 p^2}\right) . \tag{6.2.11}$$

Since we are interested in the infrared-divergent part of Eq. (6.2.11), one need only consider the $n = 0$ term in the first sum. Performing the sum over m and the momentum integrals, one obtains

$$\Gamma^{2,c}(0) = \frac{g^4}{4}\left(\frac{T}{2\pi^2\Lambda}\right)\left(\frac{T^2}{12} - \frac{T\Lambda}{2\pi^2}\right) . \tag{6.2.12}$$

The infrared-divergent contribution in $\Gamma^{2,c}(0)$ is given by

$$\frac{g^4 T^3}{96\pi^2\Lambda}$$

from which it follows that the contribution to $G_3(\lambda)$ from diagram (c) is

$$G_3^c(\lambda) = \frac{1}{96\pi^2\lambda} . \tag{6.2.13}$$

The contribution of diagram (b) in Fig. 6.1.1 may be written as

$$\Gamma^{2,b}(0) = \frac{g^4}{6}\left(T^2 \sum_{n=-\infty}^{\infty} \int_0^{\infty} \frac{d^3\mathbf{k}}{(2\pi)^3 k^2} \sum_{m=-\infty}^{\infty} \int_0^{\infty} \frac{d^3\mathbf{p}}{(2\pi)^3 p^2} \frac{1}{(p+k)^2}\right) \tag{6.2.14}$$

where it is understood that the propagators must be cut off in the infrared at Λ in order to integrate over the high-frequency modes. In this case, one cannot cut off the momentum integrals at Λ because each propagator must be cut off individually. To achieve this, one can choose a particular function to damp the contribution of modes satisfying $q^2 < \Lambda^2$ where q is the four-momentum flow along a particular line. A simple choice for the damping function is

$$\frac{q^2}{(q^2+\Lambda^2)}$$

which approaches 0 for $q^2 < \Lambda^2$ and approaches 1 for $q^2 > \Lambda^2$. The fact that the cutoff function used in this diagram differs from the step-function cutoff used in the other diagrams needs to be addressed. In principle, all propagators must be cut off using the same function $K(q^2/\Lambda^2)$, however, in this case we can make an exception. Since we are interested in obtaining the infrared-divergent behaviour of a graph, the behaviour in the far infrared will not be sensitive to the exact form of the cutoff function. If one is interested in computing the subleading terms of a graph, such as constants, then one must be consistent and use the same cutoff function. As a check, the following calculation was also performed using the step-function cutoff. In this case, a simple analytic expression for the coefficient C_1 could not be obtained. The coefficient is expressed as an integral, which when evaluated numerically does give an answer consistent with Eq. (6.2.27).

After substituting the damping function into Eq. (6.2.14) we obtain

$$\Gamma^{2,b}(0) = \frac{g^4}{6}\left(T^2 \sum_{n,m=-\infty}^{\infty} \int_0^{\infty} \frac{d^3\mathbf{k}}{(2\pi)^3 (k^2+\Lambda^2)} \int_0^{\infty} \frac{d^3\mathbf{p}}{(2\pi)^3 (p^2+\Lambda^2)} \frac{1}{(p+k)^2+\Lambda^2}\right) . \tag{6.2.15}$$

To study the infrared-divergent behaviour of Eq. (6.2.15), one need only consider the case when both $m = 0$ and $n = 0$ in the sum. To perform the integrals, it is convenient to express the propagators using the Schwinger parameterization[25]

which is

$$\frac{1}{q^2+\Lambda^2} = \int_0^\infty d\alpha \; e^{-\alpha(q^2+\Lambda^2)} \; . \tag{6.2.16}$$

We can also choose to introduce an ultraviolet cutoff at the scale of the temperature T and this will not affect the infrared-divergent behaviour as $\Lambda \to 0$. Incorporating the above changes, the infrared-divergent contribution from diagram (b) becomes

$$\Gamma^{2,b}(0) = \frac{g^4T^2}{6\,(2\pi)^6} \int_{1/T^2}^\infty d\alpha_1 d\alpha_2 d\alpha_3 \; e^{-\Lambda^2(\alpha_1+\alpha_2+\alpha_3)} \int_0^\infty d^3\mathbf{k} d^3\mathbf{p} \; e^{-\alpha_1\mathbf{k}^2-\alpha_2\mathbf{p}^2-\alpha_3(\mathbf{k}+\mathbf{p})^2} \; . \tag{6.2.17}$$

Performing the Gaussian momentum integrals and making the change of variables $x_i = \Lambda^2\alpha_i$ yields

$$\Gamma^{2,b}(0) = \frac{g^4T^2}{384\pi^3} \int_{\lambda^2}^\infty dx_1 dx_2 dx_3 \; \frac{e^{-(x_1+x_2+x_3)}}{(x_1x_2+x_1x_3+x_2x_3)^{3/2}} \tag{6.2.18}$$

where $\lambda = \Lambda/T$. If we define the function

$$A\left(\lambda^2\right) = \int_{\lambda^2}^\infty dx_1 dx_2 dx_3 \; \frac{e^{-(x_1+x_2+x_3)}}{(x_1x_2+x_1x_3+x_2x_3)^{3/2}} \tag{6.2.19}$$

we can determine the small λ behaviour but studying $\frac{\partial A(\lambda^2)}{\partial\lambda^2}$.

Taking the derivative with respect to λ^2 and making the change of variables $y_i = x_i/\lambda^2$, we find that

$$\frac{\partial A\left(\lambda^2\right)}{\partial\lambda^2} = -\frac{3}{\lambda^2} \int_1^\infty dy_1 dy_2 \; \frac{e^{-(y_1+y_2+1)\lambda^2}}{(y_1y_2+y_1+y_2)^{3/2}} \tag{6.2.20}$$

which in the limit $\lambda^2 \to 0$ is equal to

$$\frac{\partial A\left(\lambda^2\right)}{\partial\lambda^2} = -\frac{3}{\lambda^2} \int_1^\infty dy_1 dy_2 \; \frac{1}{(y_1y_2+y_1+y_2)^{3/2}} \left(1+\mathcal{O}\left(\lambda^2\right)\right) \; . \tag{6.2.21}$$

The integrals in Eq. (6.2.21) can be evaluated exactly to yield

$$\frac{\partial A\left(\lambda^2\right)}{\partial\lambda^2} = -\frac{2\pi}{\lambda^2}\left(1+\mathcal{O}\left(\lambda^2\right)\right) \tag{6.2.22}$$

which implies that the small λ behaviour of $A(\lambda^2)$ is given by

$$A\left(\lambda^2\right) = -2\pi \log\left(\lambda^2\right) + \mathcal{O}\left(\lambda^0\right) \ . \tag{6.2.23}$$

By substituting Eq. (6.2.23) into Eq. (6.2.18), one finds that the small λ divergent behaviour of $\Gamma^{2,b}(0)$ is

$$\Gamma^{2,b}\left(0\right) = -\frac{g^4 T^2}{96\pi^2} \log\left(\lambda\right) \ . \tag{6.2.24}$$

This implies that the contribution to $G_3(\lambda)$ from diagram (b) is

$$G_3^b\left(\lambda\right) = -\frac{1}{96\pi^2} \log\left(\lambda\right) \ . \tag{6.2.25}$$

Summing Eq. (6.2.13) and Eq. (6.2.25) gives the function $G_3(\lambda)$, which is found to be

$$G_3\left(\lambda\right) = -\frac{1}{96\pi^2} \log\left(\lambda\right) + \frac{1}{96\pi^2 \lambda} \ . \tag{6.2.26}$$

The coefficient C_1 may now be determined by using Eq. (6.2.26) and Eq. (6.2.10) to yield

$$C_1 = \frac{1}{96\pi^2} \ . \tag{6.2.27}$$

6.2.2. The Final Result

The expression for $S_2(z)$ is given by

$$S_2\left(z\right) = \frac{z}{64\pi^3} + \frac{1}{96\pi^2} \log\left(z\right) + C_2 + \mathcal{O}\left(1/z\right) \ . \tag{6.2.28}$$

To obtain the two-point function at zero momentum to $\mathcal{O}(g^4)$, simply substitute Eq. (6.2.28) into Eq. (6.2.6) and drop all terms of $\mathcal{O}(g^5)$ and higher. The result for the two-point function is

$$\frac{\Gamma^2\left(0\right)}{T^2} = -\frac{g^2}{24} + \frac{\mu g^2}{8\pi} + \frac{g^4 z}{64\pi^3} - \frac{g^4}{96\pi^2} \log\left(\mu\right) + g^4 \left(\frac{1}{16\pi^4} + C_2\right) + \mathcal{O}\left(g^5, z^2\right) \ . \tag{6.2.29}$$

Using the fact that $z = \lambda/\mu$ and that μ can be expanded as

$$\mu = \frac{g}{\sqrt{24}} \left(1 - \frac{3gz}{\sqrt{24}\pi^2} + \mathcal{O}\left(g^2, z\right)\right) \ , \tag{6.2.30}$$

one finds

$$\frac{\Gamma^2\left(0\right)}{T^2} = -\frac{g^2}{24} + \frac{g^3}{8\pi\sqrt{24}} - \frac{g^4}{96\pi^2} \log\left(\frac{g}{\sqrt{24}}\right) + g^4 D + \mathcal{O}\left(g^5\right) \tag{6.2.31}$$

where D is a constant. Therefore, the induced thermal mass at $\mathcal{O}(g^4)$ is

$$m^2(g,T) = \frac{g^2T^2}{24}\left(1 - \frac{3m_0}{\pi T}\right) + \left(\frac{gm_0}{2\pi}\right)^2 \log\left(\frac{m_0}{T}\right) + g^4T^2E + \mathcal{O}\left(g^5\right) \quad (6.2.32)$$

where m_0 is defined by Eq. (5.1.5) and E is a constant. The form of the result given in Eq. (6.2.32) agrees with that found by Parwani[18] who computed the mass to $\mathcal{O}(g^4)$ by explicit evaluation of the Feynman graphs. The value obtained for the constant E is given by

$$E = \frac{\alpha}{384\pi^2}$$

where the constant $\alpha = 8.8865...$ was determined using numerical methods. Although the renormalization-group approach does not yield the value of the integration constant, the nonanalytic contribution to the mass at $\mathcal{O}(g^4)$ is obtained. This is useful because in the small-coupling limit the logarithmic term will dominate the g^4T^2E term.

The effective-Lagrangian approach allowed us to determine the thermal mass to $\mathcal{O}(g^4)$ in a clean and simple fashion. At all points in the calculation, one has control over the relative sizes of terms being included and neglected. This method can be of use to check the validity of long calculations and to help settle disputes over a particular result[14]. To further illustrate the utility of these techniques, the temperature-dependent effective potential of a scalar field with spontaneous symmetry breaking will be considered in the next chapter.

Chapter 7.
The Finite-Temperature Effective Potential

In this chapter, we consider a scalar theory in which the symmetry $\phi \to -\phi$ is spontaneously broken by a negative mass squared term in the Lagrangian. The Lagrangian is symmetric under the transformation described, however, the vacuum or ground state is not. Our goal is to compute the effective potential of the system to $\mathcal{O}(1/g)$ in a clear and systematic fashion by using the power-counting procedures developed in the previous chapters. We will then compare our result with the literature and then study the behaviour of the effective potential as a function of the temperature.

7.1. Scalar Theory with a Spontaneously-Broken Symmetry

The system that is considered in this chapter is described by the following Lagrangian density:

$$\mathcal{L} = -\frac{1}{2}\partial_\mu\phi\partial^\mu\phi - V(\phi) \tag{7.1.1}$$

where the classical potential $V(\phi)$ is given by

$$V(\phi) = \frac{1}{2}m_0^2\phi^2 + \frac{1}{4!}g^2\phi^4 \,. \tag{7.1.2}$$

Notice that the Lagrangian density given by Eq. (7.1.1) is invariant under the transformation $\phi \to -\phi$. If $m_0^2 \geq 0$ then the minimum of $V(\phi)$ (which is the ground state or vacuum of the system) lies at $\phi = 0$ which is also invariant under the transformation $\phi \to -\phi$. On the other hand, if $m_0^2 = -c^2$ where c is a positive quantity, then the potential $V(\phi)$ has two minima each of which can serve as the vacuum of the theory. The symmetry $\phi \to -\phi$ of the original theory is said to be broken since the ground state of the theory is no longer invariant under that transformation.

In order to compute the effective potential using perturbation theory, we will use the method described in section 2.1.5. The first step is to perform a shift in the field ϕ where $\phi \to v + \phi$ with v a position independent quantity. One must then

subtract the ϕ-indepedent terms to keep the vacuum energy at zero. Finally, all terms linear in ϕ are eliminated to remove the tadpole contributions. The shifted Lagrangian density of the theory as defined by Eq. (2.1.37) is given by

$$\mathcal{L}_s = -\frac{1}{2}\partial_\mu\phi\partial^\mu\phi - \frac{1}{2}m^2(v)\,\phi^2 - \frac{1}{3!}g^2v\phi^3 - \frac{1}{4!}g^2\phi^4 \tag{7.1.3}$$

with

$$m^2(v) = \frac{g^2v^2}{2} - c^2\,. \tag{7.1.4}$$

This is the shifted Lagrangian density from which the effective potential will be computed.

At the classical minimum of the potential, given by Eq. (7.1.2), the expectation value of the field is $v = \pm\frac{c\sqrt{6}}{g}$ thus the masses of the scalar particles are $m^2(v) = 2c^2$ in the shifted theory. It is important to note that the theory described by Eq. (7.1.3) is not invariant under the transformation $\phi \to -\phi$. We would now like to compute the effective potential of the original theory by using the shifted Lagrangian density. The tree-level contribution to the effective potential is simply

$$V^0_{eff}(v) = -\frac{c^2}{2}v^2 + \frac{g^2}{4!}v^4\,. \tag{7.1.5}$$

The corrections to the tree-level terms are described in section 2.1.5. These corrections can be evaluated by using the loop expansion with the Feynman rules derived from the shifted Lagrangian density Eq. (7.1.3).

The vacuum expectation value of ϕ is of $\mathcal{O}(1/g)$. Thus v may be written as

$$v = \frac{c}{g}\hat{v} \tag{7.1.6}$$

where $\hat{v}$ is a dimensionless parameter of $\mathcal{O}(1)$. By substituting Eq. (7.1.6) into Eq. (7.1.5) it is easy to see that the tree-level potential is of $\mathcal{O}(1/g^2)$. To evaluate the effective potential to $\mathcal{O}(1/g)$ systematically, it is necessary to estimate the sizes of the contributions from the various diagrams. This can be achieved very efficiently by using an effective-Lagrangian approach. As before, one can first "integrate out" the high-frequency modes in the theory described by Eq. (7.1.3) and then use the low-energy effective theory to compute the quantity of interest, which in this case

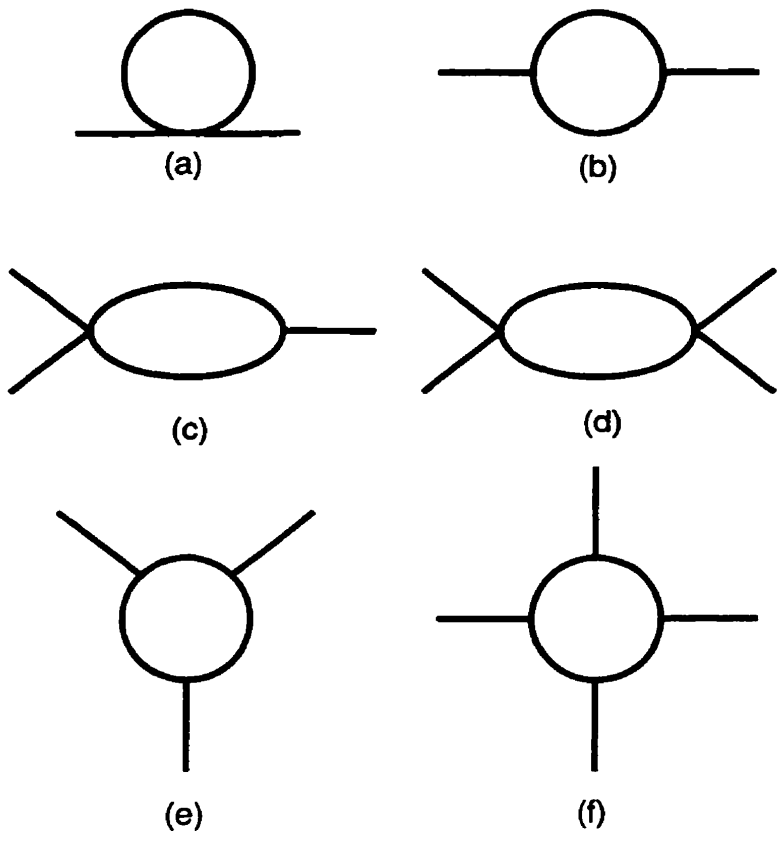

Figure 7.2.1: One-loop corrections to the tree-level vertices.

is the effective potential. Therefore, the first step in this investigation is to derive an effective-Lagrangian for the system described by Eq. (7.1.3).

7.2. Deriving The Effective Theory

The Lagrangian density for the system we are interested in is given by

$$\mathcal{L}_s = -\frac{1}{2}\partial_\mu\phi\partial^\mu\phi - \frac{1}{2}m^2(v)\,\phi^2 - \frac{1}{3!}g^2v\phi^3 - \frac{1}{4!}g^2\phi^4\,. \tag{7.2.1}$$

Once again, we choose to integrate over all modes with $p^2 > \Lambda^2$ with the cutoff Λ chosen to satisfy $gT \ll \Lambda < T$. To derive the effective theory accurate to $\mathcal{O}(g^2)$, all that is required is that the high-energy modes be integrated over in diagram (a) displayed in Fig. 7.2.1. All other one-loop corrections displayed in Fig. 7.2.1 are of $\mathcal{O}(g^4)$ and higher.

The tree-level contribution to the two-point function in the effective theory is given by

$$\Gamma^2_\Lambda(0) = -m^2(v) - \frac{g^2T}{2}\sum_{n=-\infty}^{\infty}\int_\Lambda^\infty \frac{d^3\mathbf{k}}{(2\pi)^3}\frac{1}{k^2+m^2(v)} \tag{7.2.2}$$

where the lower limit of integration represents the fact that only high-energy modes are integrated over. If we assume that $\Lambda \gg m(v)$ then Eq. (7.2.2) can be expanded as

$$\Gamma^2_\Lambda(0) = -m^2(v) - \frac{g^2T^2}{24} + \frac{g^2T\Lambda}{4\pi^2} + \mathcal{O}\left(g^2m^2(v)\right) . \tag{7.2.3}$$

Thus the effective mass in the low-energy theory is

$$m^2(v,T,\Lambda) = m^2(v) + \frac{g^2T^2}{24} - \frac{g^2T\Lambda}{4\pi^2} + \mathcal{O}\left(g^2m^2(v)\right) . \tag{7.2.4}$$

This above calculation is also valid when $m^2(v) < 0$. This is because we are integrating over modes with energies much greater than $|m(v)|$. This is an important point since we will study the effective potential for values of v where $m^2(v) < 0$. Since we are interested in studying the effective potential near the critical temperature, we can assume that the temperature is very high and rewrite it as

$$T = \frac{c}{g}\hat{t} \tag{7.2.5}$$

where $\hat{t}$ is a dimensionless parameter of $\mathcal{O}(1)$. Using the fact that $m^2(v) = g^2v^2/2 - c^2$ and that $v = \hat{v}c/g$ we find that

$$m^2(\hat{v}) = c^2\left(\frac{\hat{v}^2}{2} - 1\right) \tag{7.2.6}$$

which shows that $m^2(v)$ can also be represented by c^2 multiplied by a dimensionless parameter of $\mathcal{O}(1)$. In order to maintain perturbative calculability in the high-energy theory, we must also choose that the cutoff Λ be given by

$$\Lambda = \frac{c}{g}\hat{\lambda} \tag{7.2.7}$$

where $\hat{\lambda}$ is a dimensionless parameter. The cutoff must be chosen in this fashion to prevent the breakdown of the perturbative expansion due to the severe infrared divergences found in the ring graphs, as described in chapter four. As in the previous

chapters, we choose the cutoff such that $\Lambda \gg gT$. Finally, one can define the dimensionless parameter z in a manner similar to that used in chapters five and six as

$$z = \frac{\Lambda}{m(v, T, \Lambda)} . \tag{7.2.8}$$

By substituting Eq. (7.2.5) and Eq. (7.2.8) into Eq. (7.2.4) it is easy to verify that the leading corrections to the two-point function are of the same order as $m^2(v)$ and therefore cannot be neglected when the temperature T is near T_c. The corrections of $\mathcal{O}(g^2 m^2(v))$ are suppressed by powers of the coupling and may be neglected. At this point, one can also verify that diagram (b) in Fig. 7.2.1 does not contribute to this order when both v and T are of $\mathcal{O}(1/g)$.

Therefore the Lagrangian density for the low-energy effective theory is given by

$$\mathcal{L}_s(\Lambda, T) = -\frac{1}{2}\partial_\mu\phi\partial^\mu\phi - \frac{1}{2}m^2(v, \Lambda, T)\,\phi^2 - \frac{1}{3!}g^2 v\phi^3 - \frac{1}{4!}g^2\phi^4 + \mathcal{O}(g^4) . \tag{7.2.9}$$

The effective potential can be calculated using the theory described by Eq. (7.2.9). In the next section we estimate the sizes of the contributions to the effective potential from various graphs. This will be done for both the high-energy and low-energy theories so that the potential can be evaluated in a consistent fashion.

7.3. Next-To-Leading Order Contributions to the Effective Potential

In this section, the Feynman diagrams needed to calculate the next-to-leading order contributions to the effective potential are determined. First the diagrams that need to be considered in the high-energy theory are presented. The graphs that need to be evaluated in the effective theory are presented last.

7.3.1. The High-Frequency Contribution

The tree-level effective potential for the high-energy theory is given by Eq. (7.1.5). The high-frequency contributions are calculated by integrating over the high-energy modes in the Feynman diagrams which contribute to the effective potential. One can treat the interaction terms in Eq. (7.2.1) as being four-point interactions involving the field ϕ and a new field v. The effective potential is given by the sum of all diagrams with the field v on an external leg and with the field ϕ integrated over.

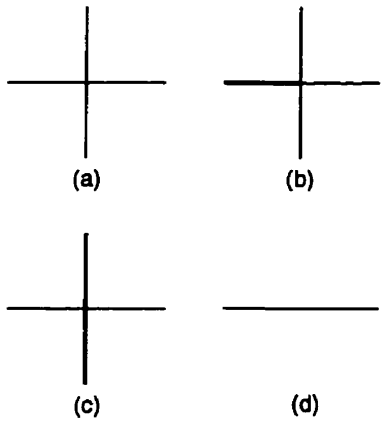

Figure 7.3.1: Interaction vertices in the shifted theory. The thin lines represent the field ϕ and the heavy lines represent the field v.

These interactions are displayed in Fig. 7.3.1. Diagram (a) represents the four-point interaction for the field ϕ. Diagram (b) is the vertex for the interaction of three ϕ's and one v. Similarly, diagram (c) is the vertex for the interaction of two ϕ's and two v's. Finally, diagram (d) is the two-point vertex for the ϕ field. There is no kinetic term for v and therefore no corresponding two-point vertex.

A diagram which contributes to the effective potential has the following general form:

$$\mathcal{V}_{HE} \approx v^{2V_2+V_3} g^{2(V_2+V_3+V_4)} \left(T \int_\Lambda d^3\mathbf{k}\right)^L \left(\frac{1}{k^2+m^2(v)}\right)^P \tag{7.3.1}$$

where V_2 represents the number of vertices with two ϕ's, V_3 is the number of vertices with three ϕ's, and V_4 is the number of vertices with four ϕ's. The number of loops in the diagram is given by L and the number of propagators is given by P. Only the $n = 0$ term in the Matsubara sum is considered and the integration is cut off in the infrared at Λ to ensure that only the high-frequency modes are integrated over. Eq. (7.3.1) can be simplified by using the fact that

$$P = V_2 + \frac{3}{2}V_3 + 2V_4 \tag{7.3.2}$$

and that

$$L = P - (V_2 + V_3 + V_4 - 1) \ . \tag{7.3.3}$$

Incorporating the above relationships, we find that

$$\mathcal{V}_{HE} \approx v^n g^{n+2L-2} \left(T \int_\Lambda d^3\mathbf{k} \right)^L \left(\frac{1}{k^2 + m^2(v)} \right)^{\frac{n}{2}+2L-2} \tag{7.3.4}$$

where n is the number of explicit v's and must be even. Using dimensional analysis, we can estimate Eq. (7.3.4) as one integral to obtain:

$$\mathcal{V}_{HE} \approx v^n g^{n+2L-2}\ T^L \int_\Lambda \mathbf{k}^{3L-1} d\mathbf{k} \left(\frac{1}{\mathbf{k}^2 + m^2(v)} \right)^{\frac{n}{2}+2L-2} . \tag{7.3.5}$$

Since we are interested in obtaining an estimate of the most infrared-divergent contribution from a particular graph, one can neglect the factor of $m^2(v)$ in the propagator since $\Lambda > m(v)$. One can also cutoff the integral in the ultraviolet at the scale T. Using these facts and performing the integral yields

$$\mathcal{V}_{HE} \approx v^n g^{n+2L-2} T^L \Lambda^{4-n-L} . \tag{7.3.6}$$

We may now substitute Eq. (7.2.5), Eq. (7.1.5) and Eq. (7.2.7) into Eq. (7.3.6) to find

$$\mathcal{V}_{HE} \approx c^4 \hat{v}^n \hat{t}^L \hat{\lambda}^{4-n-L} g^{n+2L-6} . \tag{7.3.7}$$

As already mentioned, the tree-level contribution to the effective potential is of $\mathcal{O}(1/g^2)$. One can now use Eq. (7.3.7) to determine what other diagrams may contribute to this order and to $\mathcal{O}(1/g)$. For $n = 0$ there is the possibilitity of a $\mathcal{O}(1/g^2)$ contribution when $L = 2$. When $n = 2$ there is also the possibility of a $\mathcal{O}(1/g^2)$ contribution when $L = 1$. All other contributions are of $\mathcal{O}(g^0)$ or higher. These are the only diagrams that need to be evaluated in the high-energy theory, however, since we do have an explicit expression for summing all one-loop diagrams, we will perform the complete sum and then neglect the contributions of a higher order. This also aids in streamlining the calculation since the complete one-loop sum must be performed in the low-energy effective theory. The diagrams that will be evaluated in the high-energy theory are illustrated in Fig. 7.3.2.

The first diagram in Fig. 7.3.2 represents the $L = 2$ contribution with no external field v. The second diagram is the $L = 1$ contribution with two external fields v. It is important to note that this analysis is also valid for values of v where $m^2(v) < 0$. This is the case since one can always choose the cutoff to satisfy $\Lambda > |m(v)|$.

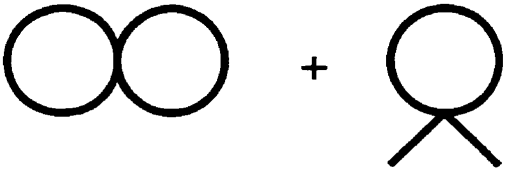

Figure 7.3.2: Contributions to the effective potential from the high-energy theory. The external lines are v's.

7.3.2. The Low-Frequency Contribution

To estimate the largest possible contributions to the effective potential from diagrams evaluated in the low-energy theory one can simply change the limits of integration in Eq. (7.3.5). Therefore the generic behaviour of diagrams in the low-energy effective theory is given by

$$\mathcal{V}_{LE} \approx v^n g^{n+2L-2}\ T^L \int_0^{\Lambda} \mathbf{k}^{3L-1} d\mathbf{k} \left(\frac{1}{\mathbf{k}^2 + m^2(v,\Lambda,T)} \right)^{\frac{n}{2}+2L-2} . \tag{7.3.8}$$

In this case, one cannot neglect the effective mass $m(v,\Lambda,T)$ because one is integrating over the low-energy modes. As was done in chapters five and six, we can scale out the effective mass $m(v,\Lambda,T)$ from the integral and obtain

$$\mathcal{V}_{LE} \approx v^n g^{n+2L-2}\ \left(\frac{T}{m(v,\Lambda,T)} \right)^L m(v,\Lambda,T)^{4-n} \int_0^{z} x^{3L-1} dx \left(\frac{1}{x^2+1} \right)^{\frac{n}{2}+2L-2} . \tag{7.3.9}$$

After rewriting the dimensionless integral as $S(z)$ and making the substitutions for v and T in terms of the dimensionless parameters $\hat{v}$ and $\hat{t}$, Eq. (7.3.9) becomes

$$\mathcal{V}_{LE} \approx \frac{c^n \hat{v}^n m(v,\Lambda,T)^{4-n}}{g^2} \left(\frac{c\hat{t}g}{m(v,\Lambda,T)} \right)^L S(z) . \tag{7.3.10}$$

From Eq. (7.3.10) it is easy to see that in order for higher-loop diagrams to be suppressed by factors of g, the effective mass $m(v,\Lambda,T)$ must satisfy $|m(v,\Lambda,T)| > \mathcal{O}(gc)$. Recall that to leading order $m^2(v,\Lambda,T) = c^2(\hat{v}^2/2 - 1 + \hat{t}^2/24 - \hat{t}\hat{\lambda}/4\pi^2)$, thus the possibility exists that the effective mass could be of $\mathcal{O}(gc)$ for specific values of $\hat{v}$ and $\hat{t}$. Therefore our expression for the effective potential is not reliable for

values of $\hat{v}$ and $\hat{t}$ which satisfy $|\hat{v}^2/2 - 1 + \hat{t}^2/24 - \hat{t}\hat{\lambda}/4\pi^2| \leq \mathcal{O}(g^2)$. This is similar to the problem of critical behaviour in three dimensions where the renormalized or physical mass vanishes at the critical temperature. In our case, it is the vanishing of the effective mass that invalidates the perturbative expansion in a region of the parameter space. Therefore the perturbative expansion is not valid for all values of $\hat{t}$ and $\hat{v}$ given a value of $\hat{\lambda}$.

It is now a trivial task to determine which diagrams need to be computed in the effective theory. Using Eq. (7.3.10), it is easy to see that all one-loop diagrams in the low-energy theory can in principle contribute to $\mathcal{O}(1/g)$. Thus we need to sum all one-loop contribtions with n-external lines in the effective theory. As already stated, this sum can be performed exactly and is presented in chapter two. One can now proceed to evaluate the effective potential to $\mathcal{O}(1/g)$.

7.4. Calculation of the Effective Potential

The tree-level contribution to the effective potential is

$$V^0_{tree}(v) = -\frac{c^2}{2}v^2 + \frac{g^2}{4!}v^4 \,. \tag{7.4.1}$$

To this we must add the contribution from the high-energy modes as discussed in the previous section. The contribution from the infinite sum of one-loop diagrams is given by

$$V^1_{he}(v) = \frac{T}{2}\sum_{n=-\infty}^{\infty}\int_{\Lambda}^{\infty}\frac{d^3\mathbf{k}}{(2\pi)^3}\log\left(k^2 + m^2(v)\right) \tag{7.4.2}$$

where the lower limit of integration ensures that one integrates over the high-frequency modes. After performing the sum and making a high-temperature expansion in $m(v)/T$, one obtains

$$\begin{aligned} V^1_{he}(v) =& \frac{m^2(v)T^2}{24} - \frac{m^3(v)T}{12\pi} - \frac{T\Lambda^3}{12\pi^2}\log\left(\Lambda^2 + m^2(v)\right) + \frac{T\Lambda^3}{18\pi^2} - \frac{m^2(v)T\Lambda}{6\pi^2} \\ &+ \frac{m^3(v)T}{6\pi^2}\arctan\left(\frac{\Lambda}{m(v)}\right) + \mathcal{O}\left(g^0\right) \,. \end{aligned} \tag{7.4.3}$$

All the terms that have been neglected are of $\mathcal{O}(g^0)$ and higher. These terms include both temperature-dependent and vacuum contributions to the effective potential.

Interested readers may find the explicit expression for the vacuum contribution in the paper by Carrington[48]. The contribution from the two-loop graph is given by

$$V_{he}^{2}(v) = \frac{g^2}{8}\left(T\sum_{n=-\infty}^{\infty}\int_{\Lambda}^{\infty}\frac{d^3\mathbf{k}}{(2\pi)^3}\frac{1}{k^2+m^2(v)}\right)^2 \tag{7.4.4}$$

which can be expanded as

$$V_{he}^{2}(v) = \frac{g^2}{8}\left(\frac{T^2}{12}-\frac{T\Lambda}{2\pi^2}+\mathcal{O}\left(m^2(v)\right)\right)^2 . \tag{7.4.5}$$

One can neglect the T^4 term because it is independent of v and therefore does not contribute to the effective potential. One can also neglect the v-independent terms that are function of Λ, however, we will keep these terms to show that the cutoff dependence does in fact cancel. Adding the above expressions for $V_{he}^{1}(v)$ and $V_{he}^{2}(v)$ yields

$$\begin{aligned} V_{he}(v) =& \frac{m^2(v)T^2}{24}-\frac{m^3(v)T}{12\pi}-\frac{T\Lambda^3}{12\pi^2}\log\left(\Lambda^2+m^2(v)\right)+\frac{T\Lambda^3}{18\pi^2}-\frac{m^2(v)T\Lambda}{6\pi^2} \\ &+\frac{m^3(v)T}{6\pi^2}\arctan\left(\frac{\Lambda}{m(v)}\right)-\frac{g^2T^3\Lambda}{96\pi^2}+\frac{g^2T^2\Lambda^2}{32\pi^4}+\mathcal{O}\left(g^0\right) . \end{aligned} \tag{7.4.6}$$

The contribution to the effective potential from the low-energy theory is also given by the sum of all one-loop graphs. Thus one can write

$$V_{le}^{1}(v) = \frac{T}{2}\int_{0}^{\Lambda}\frac{d^3\mathbf{k}}{(2\pi)^3}\log\left(k^2+m^2(v,\Lambda,T)\right) . \tag{7.4.7}$$

After the integral is evaluated, one obtains

$$\begin{aligned} V_{le}^{1}(v) =& \frac{T\Lambda^3}{12\pi^2}\log\left(\Lambda^2+m^2(v,\Lambda,T)\right)-\frac{T\Lambda^3}{18\pi^2}+\frac{m^2(v,\Lambda,T)T\Lambda}{6\pi^2} \\ &-\frac{m^3(v,\Lambda,T)T}{6\pi^2}\arctan\left(\frac{\Lambda}{m(v,\Lambda,T)}\right) . \end{aligned} \tag{7.4.8}$$

The complete expression for the effective potential accurate to $\mathcal{O}(1/g)$ is obtained by adding Eq. (7.4.1), Eq. (7.4.6) and Eq. (7.4.8). After adding the three equations,

we arrive at

$$V(v) = -\frac{c^2}{2}v^2 + \frac{g^2}{4!}v^4 + \frac{m^2(v)T^2}{24} - \frac{m^3(v)T}{12\pi} - \frac{m^2(v)T\Lambda}{6\pi^2} - \frac{g^2T^3\Lambda}{96\pi^2} + \frac{g^2T^2\Lambda^2}{32\pi^4} + \frac{m^3(v)T}{6\pi^2}\arctan\left(\frac{\Lambda}{m(v)}\right) + \frac{T\Lambda^3}{12\pi^2}\log\left(\frac{\Lambda^2+m^2(v,\Lambda,T)}{\Lambda^2+m^2(v)}\right) + \frac{m^2(v,\Lambda,T)T\Lambda}{6\pi^2} - \frac{m^3(v,\Lambda,T)T}{6\pi^2}\arctan\left(\frac{\Lambda}{m(v,\Lambda,T)}\right) + \mathcal{O}(g^0) \ . \tag{7.4.9}$$

Eq. (7.4.9) can be greatly simplified by expanding the logarithm and arctangent functions and dropping all terms of $\mathcal{O}(g^0)$ and higher. The first term on the second line of Eq. (7.4.9) may be expanded as

$$\frac{m^3(v)T}{6\pi^2}\arctan\left(\frac{\Lambda}{m(v)}\right) = \frac{m^3(v)T}{12\pi} + \mathcal{O}(g^0) \ . \tag{7.4.10}$$

The second term on the second line of Eq. (7.4.9) may be written as

$$\frac{T\Lambda^3}{12\pi^2}\log\left(\frac{\Lambda^2+m^2(v,\Lambda,T)}{\Lambda^2+m^2(v)}\right) = \frac{T\Lambda^3}{12\pi^2}\left(\frac{g^2T^2}{24} - \frac{g^2T\Lambda}{4\pi^2}\right)\left(\frac{1}{\Lambda^2}\right) + \mathcal{O}(g^0) \tag{7.4.11}$$

where we have used Eq. (7.2.4) for $m^2(v,\Lambda,T)$. Finally, the first term on line three of Eq. (7.4.9) may be written as

$$\frac{m^2(v,\Lambda,T)T\Lambda}{6\pi^2} = \frac{m^2(v)T\Lambda}{6\pi^2} + \frac{g^2T^3\Lambda}{144\pi^2} - \frac{g^2T^2\Lambda^2}{24\pi^4} + \mathcal{O}(g^0) \ . \tag{7.4.12}$$

Substituting the above expressions into Eq. (7.4.9) we find that all polynomials that are linear in Λ cancel. The terms that have quadratic Λ dependence do not cancel, however, these terms can be rewritten using the definition of z as terms of $\mathcal{O}(g^0, z^2)$ which can be neglected. The effective potential can now be written as

$$V(v) = -\frac{c^2}{2}v^2 + \frac{g^2}{4!}v^4 + \frac{m^2(v)T^2}{24} - \frac{m^3(v,\Lambda,T)T}{6\pi^2}\arctan(z) + \mathcal{O}(g^0, z^2) \tag{7.4.13}$$

where it is understood that we are interested in the large z limit. One further simplification can be made by expanding $m^3(v,\Lambda,T)$ in the following manner:

$$m^3(v,\Lambda,T) = \left(m^2(v) + \frac{g^2T^2}{24}\right)^{\frac{3}{2}}(1 + \mathcal{O}(g,z)) \ . \tag{7.4.14}$$

Thus our final expression for the effective potential, accurate $\mathcal{O}(1/g)$, is given by

$$V(v) = -\frac{c^2}{2}v^2 + \frac{g^2}{4!}v^4 + \frac{m^2(v)T^2}{24} - \frac{m^3(v,T)T}{12\pi}(1 + \mathcal{O}(1/z)) + \mathcal{O}(g^0) \tag{7.4.15}$$

where $m^2(v,T) = m^2(v) + g^2T^2/24$ and we have expanded about large z. This expression agrees with the results found in the literature[48,49–51] in the limit $z \to \infty$.

An important point is that our derivation makes it clear when our expression is valid, with the variables T, Λ, and $m(v,\Lambda,T)$ subject to certain constraints. The constraints that must be satisfied are $T > \Lambda \gg |m(v,\Lambda,T)| > \mathcal{O}(gc)$ with the coupling constant $g \ll 1$. These conditions are not made explicit in the papers by Carrington[48] and Takahashi[50]. This lack of contraints on the validity of the perturbative expansion leads to incorrect conclusions concerning the nature of the phase transition. The paper by Espinosa[49] does have constraints, however, it involves the introduction of the three new expansion parameters. The effective-Lagrangian approach simplifies the task of estimating the sizes of contributions since the expansion parameter is always the coupling constant. We will now study the behaviour of Eq. (7.4.15) as a function of v and T keeping in mind that the above-mentioned constraints must be satisfied.

7.5. The Effective Potential as a Function of Temperature

It is useful to rewrite Eq. (7.4.15) as a dimensionless function before studying the behaviour of the result. Using Eq. (7.1.5), Eq. (7.2.5), Eq. (7.2.6), Eq. (7.2.7) and Eq. (7.2.8) we find that

$$\frac{g^2V(v)}{c^4} = -\frac{\hat{v}^2}{2} + \frac{\hat{v}^4}{4!} + \frac{\hat{v}^2\hat{t}^2}{48} - \frac{g\left(\hat{v}^2/2 - 1 + \hat{t}^2/24\right)^{\frac{3}{2}}\hat{t}}{12\pi} + \mathcal{O}\left(g^2, z^2\right) \qquad (7.5.1)$$

where terms of $\mathcal{O}(1/z)$ and higher have been dropped. It is easy to see that the possibility exists that Eq. (7.5.1) can develop an imaginary part for some values of $\hat{v}$ and $\hat{t}$. At this point, we will simply study the real part of the effective potential and justify this procedure in the next section.

There are some general observations that one can make concerning Eq. (7.5.1) that can help one understand its behaviour. The right-hand side is composed of three terms. There are terms that are explicitly quadratic and quartic in $\hat{v}$ and a term that can be thought of as being cubic in $\hat{v}$. If the temperature satisfies $\hat{t} < \sqrt{24}$, then the coefficient function of the $\hat{v}^2$ is negative. Thus the potential

has a negative slope near the origin. For large values of $\hat{v}$, the quartic dominates and the potential has a positive slope. Thus the potential has one minimum at a positive value of $\hat{v}$ for temperatures $\hat{t} < \sqrt{24}$.

If the temperature is raised so that the coefficient function of the quadratic term has a small but positive value then the slope of the potential near the origin is positive. As one then probes larger values of $\hat{v}$, the slope of the potential may in fact become negative since the coefficient of the "cubic" term is explicitly negative. This happens only if the temperature is not too high. If the temperature is too high then the quadratic and quartic terms always dominate and the potential always has a positive slope. This is the case where there is one minimum at the origin. Assuming that the "cubic" term does dominate for a given range of $\hat{v}$ then we have the case of two local minima. There is a minimum at the origin and another minimum at a finite value of $\hat{v}$. If one has two degenerate minima at some temperature $\hat{t}$ then the phase transition is said to be of first order. If this does not occur, then we have a second-order phase transition.

To make a more quantitative analysis, one should study the derivative of the potential. By taking a derivative with respect to $\hat{v}$, one can determine the number and positions of the local maxima and minima. To begin, it is convenient to rewrite Eq. (7.5.1) as

$$\hat{V}(\hat{v}) = A(\hat{t})\,\hat{v}^2 - \frac{gm^3(\hat{v},\hat{t})\,\hat{t}}{12\pi} + \frac{\hat{v}^4}{24} \tag{7.5.2}$$

where $A(\hat{t}) = \hat{t}^2/48 - 1/2$. Taking a derivative with respect to $\hat{v}$ yields

$$\frac{d\hat{V}(\hat{v})}{d\hat{v}} = \hat{v}\left(2A(\hat{t}) - \frac{gm(\hat{v},\hat{t})\,\hat{t}}{8\pi} + \frac{\hat{v}^2}{6}\right) \tag{7.5.3}$$

where $\frac{\partial m}{\partial \hat{v}} = \hat{v}/2m$ is used. It follows that the maxima and minima lie at points where

$$\hat{v}\left(\hat{v}^2 - \frac{3gm(\hat{v},\hat{t})\,\hat{t}}{4\pi} + 12A(\hat{t})\right) = 0\,. \tag{7.5.4}$$

Eq. (7.5.4) shows that there is always a local extremum at $\hat{v} = 0$.

One can now study Eq. (7.5.4) to determine the conditions required for two, real, unequal roots other than $\hat{v} = 0$. We know that the temperature would be $\sqrt{24}$ if the "cubic" term were zero. For $m \neq 0$, we explore the vicinity of this

temperature by taking $\hat{t}^2 = 24 + \delta t^2$ where δt^2 is a very small positive quantity. If one substitutes this expression for the square of the temperature into Eq. (7.5.4) and makes the change of variable $m^2 = \hat{v}^2/2 + \delta t^2/24$, one obtains the following equation for the mass:

$$m^2 - \frac{3gm\hat{t}}{8\pi} + \frac{\delta t^2}{12} = 0\,. \tag{7.5.5}$$

If one makes an expansion in powers of δt^2 and neglects terms of order $g\delta t^2$ then the following quadratic equation is obtained:

$$m^2 - \frac{3g\sqrt{24}m}{8\pi} + \frac{\delta t^2}{12} = 0\,. \tag{7.5.6}$$

In order for there to be two, distinct, real roots the discriminant of Eq. (7.5.6) must be greater than zero. This must be the case since m^2 is strictly positive at this temperature. This implies that

$$\delta t^2 < \frac{81g^2}{8\pi^2}\,. \tag{7.5.7}$$

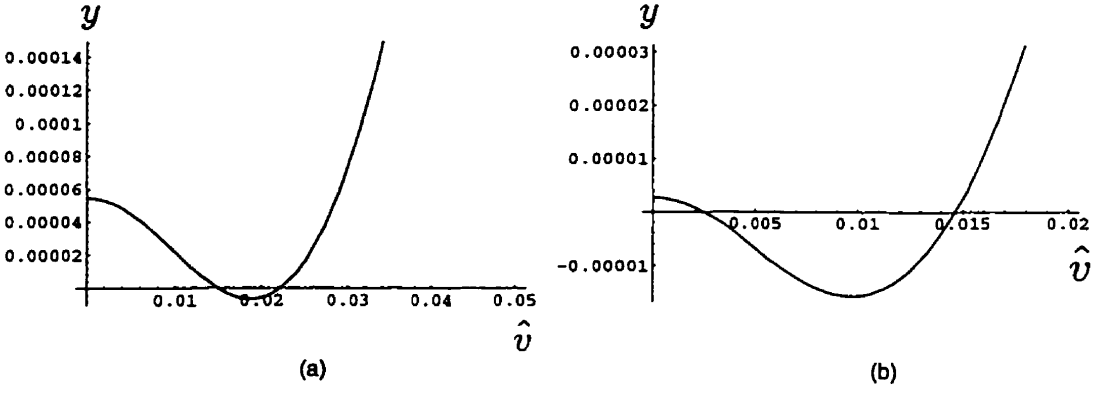

Figure 7.5.1: Graphs of Eq. (7.5.8) for two values of g and $\hat{t}$. Graph (a) is for the values $g = 0.2$ and $\hat{t} = 4.8994$. Graph (b) is for the values $g = 0.1$ and $\hat{t} = 4.899076$.

By solving the quadratic equation, it is easy to see that the roots are given by $\hat{v} \sim \mathcal{O}(g)$. One can graph the function

$$y\left(\hat{v}\right) = \hat{v}^2 - \frac{3gm\left(\hat{v},\hat{t}\right)\hat{t}}{4\pi} + 12A\left(\hat{t}\right) \tag{7.5.8}$$

for various values of g and $\hat{t}$ to verify that it passes through zero at values of $\hat{v} \neq 0$. One should also expect $|\hat{y}|$ to be at most of $\mathcal{O}(g^2)$ in the region of the roots.

In Fig. 7.5.1 we have graphed Eq. (7.5.8) for some specific values of g and $\hat{t}$ to show that it does in fact pass though zero. It is easy to verify that these values of g and $\hat{t}$ do in fact satisfy Eq. (7.5.7). Note that the positions of the roots are at values of $\hat{v} < \mathcal{O}(g)$. We can also plot the effective potential for various temperatures to see the first-order phase transition.

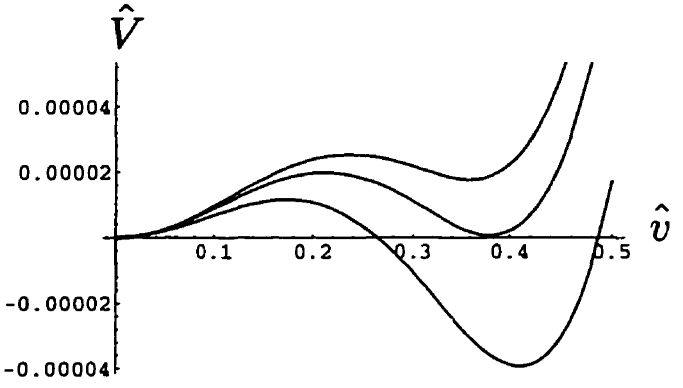

Figure 7.5.2: Graph of the effective potential given by Eq. (7.5.2). The value of the coupling constant is set at $g = 1$ and the value of the potential at the origin is set to zero. The three curves show the behaviour of the potential for various temperatures. The lower curve is for $\hat{t} = 5.003$, the middle curve is for $\hat{t} = 5.005$, and the upper curve is for $\hat{t} = 5.006$.

Evidence of a first-order phase transition in this scalar model has also been observed by Espinosa[49] et al. and by Takahashi[50]. Now that the possibility of a first-order phase transition has been established, we must determine the domain of validity of this result. The mathematical limitations of the perturbatively calculated effective potential are presented in the next section.

7.6. Mathematical Limitations of the Result

Before one can conclude whether or not a first-order phase transition exists in this model, there are some points that need to be addressed. The first point concerns the fact that $m^2(\hat{v}, \hat{\lambda}, \hat{t}) < 0$ for some values of $\hat{v}$ and $\hat{t}$. If the mass squared is negative,

this implies that the effective potential will be complex. At first, one may think that this poses a problem since it can be shown[52–53] that the effective potential should be real for all values of $\hat{v}$. The resolution[54] to this problem lies in the fact that the perturbatively-calculated effective potential can still be interpreted as a physically meaningful quantity even in situations where it becomes complex. This quantity can describe an unstable, spatially homogeneous quantum state. The imaginary part of the potential is related to the decay rate per unit volume of the system, and the real part corresponds to the internal energy density of the system. Thus for our study, we will focus on the real part of perturbatively-calculated effective potential.

The second point concerns the validity of the perturbative expansion in the low-energy effective theory. As already discussed in section 7.3, in order for the perturbative expansion to be reliable in the low-energy theory, one must demand that $|m^2(v,\Lambda,T)| > \mathcal{O}(g^2c^2)$. We know that $m^2(v,\Lambda,T)$ may be expressed as

$$m^2(v,\Lambda,T) = \left(m^2(v) + \frac{g^2T^2}{24}\right)\left(1 - \frac{g^2T\Lambda}{4\pi^2\left(m^2(v) + \frac{g^2T^2}{24}\right)} + \mathcal{O}(g^2)\right) \tag{7.6.1}$$

which can be rewritten as

$$m^2(v,\Lambda,T) = \left(m^2(v) + \frac{g^2T^2}{24}\right)\left(1 - \frac{g^2Tm(v,\Lambda,T)\,z}{4\pi^2\left(m^2(v) + \frac{g^2T^2}{24}\right)} + \mathcal{O}(g^2)\right) \tag{7.6.2}$$

by using the definition of z. After switching to the dimensionless variables, we obtain

$$m^2\left(\hat{v},\hat{\lambda},\hat{t}\right) = \left(m^2(\hat{v}) + \frac{c^2\tilde{t}^2}{24}\right)\left(1 - \frac{cg\hat{t}m\left(\hat{v},\hat{\lambda},\hat{t}\right)z}{4\pi^2\left(m^2(\hat{v}) + \frac{c^2\tilde{t}^2}{24}\right)} + \mathcal{O}(g^2)\right) . \tag{7.6.3}$$

Therefore, in order for the perturbative expansion in the low-energy theory to be valid, one must demand that

$$\left|m^2(\hat{v}) + \frac{c^2\tilde{t}^2}{24}\right| > \mathcal{O}(g^2c^2) . \tag{7.6.4}$$

Expanding $\tilde{t}^2 = 24 + \delta t^2$ near the phase transition, we find that

$$\left|\frac{\hat{v}^2}{2} + \frac{\delta\tilde{t}^2}{24}\right| > \mathcal{O}(g^2) . \tag{7.6.5}$$

From Eq. (7.5.7), we know that the condition to see the phase transition is $\delta t^2 < \mathcal{O}(g^2)$. Substituting this constraint into Eq. (7.6.5), we obtain

$$|\hat{v}| > \mathcal{O}(g) \ . \tag{7.6.6}$$

This is the condition required to maintain perturbative calculability. The expression for the effective potential, given by Eq. (7.5.1), is only valid in regions where $\hat{v} > \mathcal{O}(g)$ near the critcal temperature. As one can see in Fig. 7.5.2, the evidence for a first-order phase transition occurs for values of $\hat{v} < \mathcal{O}(g)$ since $g = 1$. Decreasing the value of g does not help one probe this region. Computing the effective-potential to a higher-order is also not helpful in studying this region. Perturbation theory is simply not rich enough to allow one to probe the nature of the phase transition. This agrees with the result that one cannot conclude purely within perturbation theory whether the phase transition is second order or weakly first order[55–56]. It has been argued that our model is in the same universality class as the three-dimensional Ising model which is known to exhibit a second order phase transition[57].

We have shown that by using an effective-Lagrangian approach one is able to reorganize the perturbative expansion in a manner that allows one to count the powers of the coupling constant in a systematic fashion. We are also able to determine the constraints that maintain perturbative calculability. With these tools, we calculated the effective potential in a scalar model with spontaneous symmetry breaking to $\mathcal{O}(1/g)$. As a consequence of employing an effective-Lagrangian approach, the fact that the order of the phase transition cannot be determined perturbatively is obtained in a natural way. Perturbation theory in the low-energy theory is not valid in the critical region. Not surprisingly, it is the vanishing of the effective mass in the low-energy theory that invalidates the perturbative expansion. The vanishing of the mass occurs in the critical region.

Chapter 8.
Conclusion

There are several aspects of this thesis that should be emphasized. First, we have shown how the reorganization of perturbation theory which is required for a hot massless scalar theory can be efficiently derived by employing an effective-Lagrangian approach. By choosing a cutoff scale Λ and integrating over all modes in the massless theory with four-momenta greater than the cutoff, one can derive an effective-Lagrangian which describes exactly the same physics. The difference between the original theory and the effective theory lies only in the description of the physics. For example, if the original theory is that of a massless scalar field with a quartic interaction then the effective theory is that of a massive scalar field with an infinite number of interactions which depend on the cutoff scale Λ. The appearance of the mass term restores perturbative calculability since it eliminates the severe infrared divergences such as those found in the original massless theory. The low-energy effective theory can be used to compute quantities to any desired order in the coupling constant by using the loop expansion. To illustrate these points, the induced thermal mass was computed to both one and two-loop order in chapters five and six. In chapter five, the next-to-leading order correction to the induced mass was computed using both the original theory and the effective theory. The calculation involved the summation of an infinite number of infrared-divergent graphs in the original theory whereas only one graph was computed in the effective theory.

The second point is that the effective-Lagrangian formulation permits the singular dependence on coupling constants in physical quantities to be determined without explicitly evaluating any Feynman graphs. This approach is used in chapter six to compute the induced thermal mass to $\mathcal{O}(g^4)$. Although nonsingular dependence on g cannot be obtained in this manner, the dominant logarithmic term is easily found. The form of the result agrees with the more complete calculations of Parwani[18]. Thus the renormalizaton-group approach can be used as a method for verifying more involved calculations.

A third important point is that the effective-Lagrangian formulation permits an efficient determination of the conditions when power counting is valid. To illustrate this, the finite-temperature effective potential was calculated to order $\mathcal{O}(1/g)$ in a scalar theory with spontaneous symmetry breaking. Although the expression obtained agrees with the literature, it cannot be concluded that the model exhibits a first-order phase transition purely within perturbation theory. The region where one observes the evidence of a first-order phase transition lies outside of the region where perturbation theory is valid. Non-perturbative methods[57,58] are required to conclude whether the phase transition is of the first or second order. This result may have some interesting consequences concerning models of electroweak baryogenesis [59–71]. It is generally accepted that a strongly first-order transition is needed to maintain the baryon asymmetry generated during the phase transition. If the transition is too weak then any asymmetry created will be washed out. It would be interesting to apply these power-counting methods and determine whether or not the evidence of a first-order phase transition persists.

Finally, the effective-Lagrangian approach promises to provide a conceptual framework for understanding other thermal Quantum Field Theories. The resummed propagators and vertices found in Braaten and Pisarski's[13] resummed hot QCD are analogous to the effective propagators and vertices that we obtained by integrating out the high-frequency modes in the scalar field theory. An interesting project would be to attempt to derive the effective action which generates the "Hard Thermal Loop" corrections[17] for hot QCD by employing the effective-Lagrangain approach.

The effective-Lagrangian approach applied to hot QCD has already proven to be a useful tool in studying the damping of energetic Quarks and Gluons[14]. It is hoped that the development of these methods will help in carrying out calculations involving low-energy or "soft" particles to higher orders. This can in turn aid in understanding the behaviour of the Quark-Gluon plasma where the emission of low-energy dileptons could signal plasma formation in relativistic heavy-ion collisions. These techniques will also be useful in determining the transport coefficients of the

plasma. Thus a greater understanding of the behaviour of matter at high temperatures can be gained by employing an effective-Lagrangian approach in studying thermal Quantum Field Theories.

And there you go.

References

1. F. Combley, Rep. Prog. Phys. 42, 1889 (1979).
2. R.P. Feynman, Quantum Electrodynamics (W.A. Benjamin Inc., New York, 1962).
3. K. Gottfried and V.F. Weisskopf, Concepts of Particle Physics Volume II (Oxford University Press Inc., New York, 1986).
4. S.L. Glashow, Nucl. Phys. 22, 579 (1961).
5. S. Weinberg, Phys. Rev. Lett. 19, 1264 (1967).
6. A. Salam, in Elementary Particle Theory, ed. N. Svartholm (Almqvist and Wiksell, Stockholm, 1968).
7. F.J. Hasert et al., Phys. Lett. 46B, 138 (1973).
8. D. Gross and F. Wilczek, Phys. Rev. D9, 980 (1974).
9. A.S. Alexandrov and N.F. Mott, High Temperature Superconductors and Other Superfluids (Taylor & Francis Ltd., 1994).
10. R.D. Pisarski, Phys. Rev. Lett. 63, 1129 (1989).
11. E. Braaten and R.D. Pisarski, Phys. Rev. Lett. 64, 1338 (1990).
12. E. Braaten and R.D. Pisarski, Phys. Rev. D42, 2156 (1990).
13. E. Braaten and R.D. Pisarski, Nucl. Phys. B337, 569 (1990).
14. C.P. Burgess and A.L Marini, Phys. Rev. D45, R17 (1992); A. Rebhan, Phys. Rev. D46, 482 (1992).
15. J. Frenkel and J.C. Taylor, Nucl. Phys. B334, 199 (1990).
16. J.C. Taylor and S.M.H. Wong, Nucl. Phys. B346, 115 (1990).
17. E. Braaten and R.D. Pisarski, Phys. Rev. D45, 1827 (1992).
18. R. Parwani, Phys. Rev. D45, 4695 (1992) with erratum in Phys. Rev. D48, 5965 (1993).
19. E. Braaten, in "Hot Summer Daze - BNL Summer Study on QCD at Nonzero Temperature and Density", eds. A. Gocksh and R. Pisarski (World Scientific, New Jersey, 1992).

20. C.P. Burgess and A.L. Marini, in "MRST '94: What Next? Exploring The Future of High-Energy Physics", eds. J.R. Cudell, K.R. Dienes and B. Margolis (World Scientific, New Jersey, 1994).

21. J. Kapusta, Finite Temperature Field Theory (Cambridge University Press, 1989).

22. A.L. Fetter and J.D. Walecka, Quantum Theory of Many-Particle Systems (McGraw-Hill Inc., 1971).

23. G. Baym and N. Mermin, Journ. Math. Phys. 2, 232 (1961).

24. T.S. Evans, Nucl. Phys. B374, 340 (1992).

25. D.J. Amit, Field Theory, the Renormalization Group, and Critical Phenomena (World Scientific, Singapore, 1984).

26. L.H. Ryder, Quantum Field Theory (Cambridge University Press, 1985).

27. L.S. Brown, Quantum Field Theory (Cambridge University Press, 1992).

28. R. Jackiw, Phys. Rev. D9, 1686 (1974).

29. T. Matsubara, Prog. Theor. Phys. 14, 351 (1955).

30. N.P. Landsman and Ch.G. van Weert, Phys. Rep. 145, 143 (1987).

31. R.D. Pisarski, Nucl. Phys. B309, 476 (1988).

32. V. Baluni, Phys. Rev. D17, 2092 (1978).

33. B.A. Freedman and L.D. McLarren, Phys. Rev. D16, 1130, 1147, 1169 (1977).

34. S. Weinberg, in "Asymptotic Realms of Physics", eds. A.H. Guth, K. Huang and R.L. Jaffe (The MIT Press, 1984).

35. K.G. Wilson, Phys. Rev. B4, 3174, 3184 (1971).

36. K.G. Wilson and J.C. Kogut, Phys. Rep. 12C, 75 (1974).

37. K.G. Wilson, Rev. Mod. Phys. 55, 583 (1983).

38. E. Braaten and A. Nieto, Phys. Rev. D51, 6990 (1995).

39. J.C. Collins, Renormalization: an introduction to renormalization, the renormalization group, and the operator-product expansion (Cambridge University Press, 1984).

40. R.L. Ingraham, Renormalization Theory of Quantum Field Theory with a Cuttoff (Gordon and Breach, New York, 1967).

41. T.R. Morris, Int. J. Mod. Phys. A9, 2411 (1994).

42. G.P. LePage, in "From Actions To Answers", eds. by T. DeGrand and D. Toussiant (World Scientific, 1990).

43. J. Polchinski, Nucl. Phys. B231, 269 (1984).

44. C.P. Burgess, Details found in the course notes entitled "An Introduction to Effective Lagrangians and their Applications", Un cours de Troisième Cycle, Lausanne, Switzerland (1995).

45. H.E. Haber and H.A. Weldon, J. Math. Phys. 23, 1852 (1982).

46. L. Dolan and R. Jackiw, Phys. Rev. D9, 3320 (1974).

47. S. Weinberg, Proceedings of the International School of Subnuclear Physics, eds. A. Zichichi (Plenum Press, 1976).

48. M.E. Carrington, Can. J. Phys. 71, 227 (1993).

49. J.R. Espinosa, M. Quiros and F. Zwirner, Phys. Lett. 291B, 115 (1992).

50. K. Takahashi, Z. Phys. C26, 601 (1985).

51. G. Amelino-Camelia and S.-Y. Pi, in "Banff/CAP Workshop on Thermal Field Theory", eds. F.C. Khanna, R. Kobes, G. Kunstatter and H. Umezawa (World Scientific, 1994).

52. K. Symanzik, Commun. Math. Phys. 16, 48 (1970).

53. J. Iliopoulos, C. Itzykson and A. Martin, Rev. Mod. Phys. 47, 165 (1975).

54. E.J. Weinberg and A. Wu, Phys. Rev. D36, 2474 (1987).

55. D.A. Kirzhnits and A.D. Linde, Ann. Phys. 101, 195 (1976).

56. P. Arnold, Phys. Rev. D46, 2628 (1992).

57. I.D. Lawrie, J. Phys. C11, 3857 (1978).

58. G. Amelino-Camelia, in "Banff/CAP Workshop on Thermal Field Theory", eds. F.C. Khanna, R. Kobes, G. Kunstatter and H. Umezawa (World Scientific, 1994).

59. M. Dine, R. Leigh,P. Huet, A. Linde and D. Linde, Phys. Rev. D46, 550 (1992).

60. V.A. Kuzmin, V.A. Rubakov and M.E. Shaposhnikov, Phys. Lett. 155B, 36 (1985).

61. M.E. Shaposhnikov, JETP Lett. 44, 465 (1986).

62. M.E. Shaposhnikov, Nucl. Phys. B287, 757 (1987).

63. M.E. Shaposhnikov, Nucl. Phys. B299, 797 (1988).

64. A.I. Bochkarev, S.Y. Khlebnikov and M.E. Shaposhnikov, Nucl. Phys. B329, 493 (1990).

65. L. McLerran, Phys. Rev. Lett. 62, 1075 (1989).

66. L. McLerran, M. Shaposhnikov, N. Turok and M. Voloshin, Phys. Lett. 256B, 451 (1991).

67. N. Turok and P. Zadrozny, Phys. Rev. Lett. 65, 2331 (1990).

68. N. Turok and P. Zadrozny, Nucl. Phys. B358, 471 (1991).

69. M. Dine, P. Huet, R. Singleton and L. Susskind, Phys. Lett. 257B, 351 (1991).

70. A. Cohen, D.B. Kaplan and A.E. Nelson, Nucl. Phys. B349, 727 (1991).

71. P. Arnold and O. Espinosa, Phys. Rev. D47, 3546 (1993).

IMAGE EVALUATION TEST TARGET (QA-3)

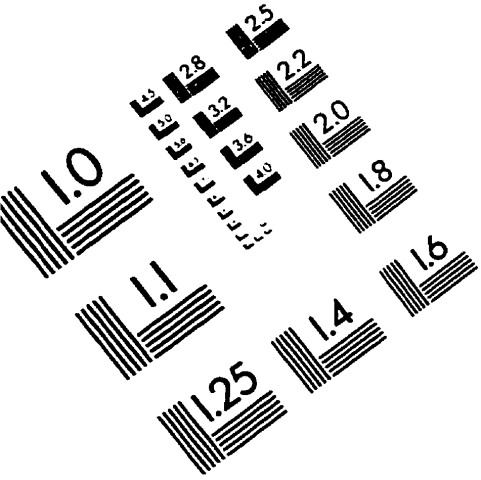

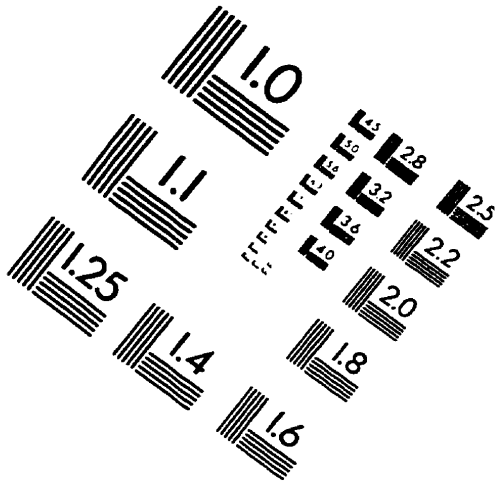

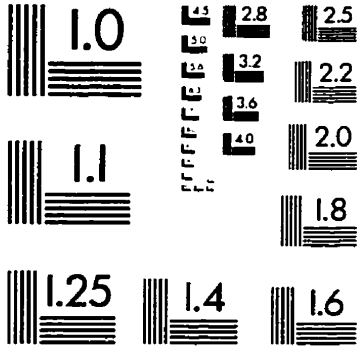

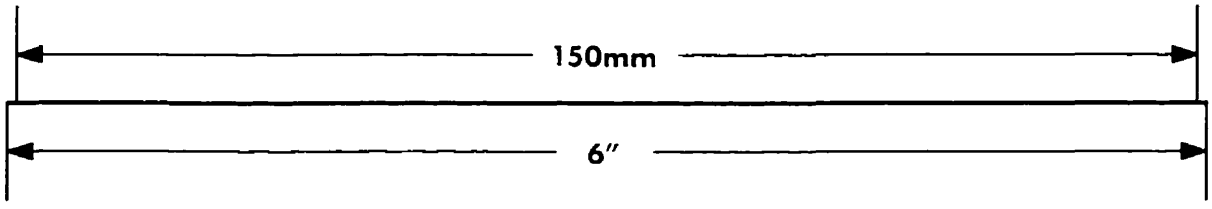

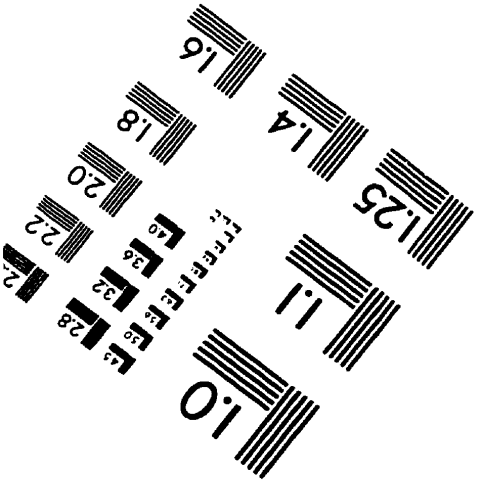

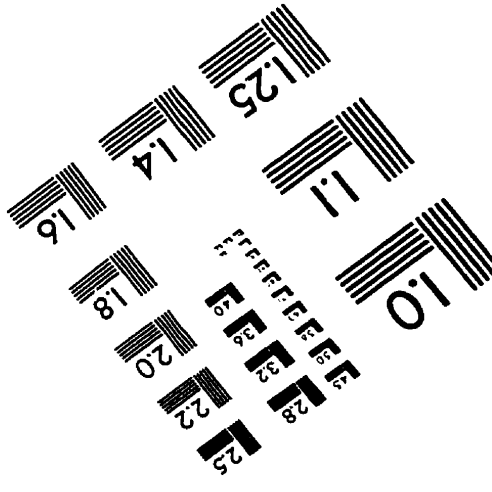

APPLIED IMAGE, Inc
1653 East Main Street
Rochester, NY 14609 USA
Phone: 716/482-0300
Fax: 716/288-5989